To the Graduate Council:

I am submitting herewith a thesis written by Daniel Aaron Lehman entitled "Viscosity Measurement Technique by Merging Liquid Drops Aboard the International Space Station". I have examined the final paper copy of this thesis for form and content and recommend that it be accepted in partial fulfillment of the requirements for the degree of Master of Science, with a major in Aerospace Engineering.

Basil N. Antar, Major Professor

We have read this thesis
And recommend its acceptance:

Accepted for the Council:

Vice Chancellor and
Dean of Graduate Studies

Thesis
2005
.L445

VISCOSITY MEASUREMENT TECHNIQUE BY MERGING LIQUID DROPS ABOARD THE INTERNATIONAL SPACE STATION

A Thesis
Presented for the
Master of Science
Degree
The University of Tennessee, Knoxville

Daniel Aaron Lehman
December 2005

For my family

ACKNOWLEDGMENTS

I would like to thank Dr. Basil Antar for everything he has done for me in the last two years. He has been: my teacher, my advisor, my mentor, and my friend. I would also like to thank Dr. Edwin Etheridge at NASA-MSFC for his help and guidance on this project. And thank Dr. Donald Reiss at NASA-MSFC who has been a lot of fun to work with at Marshall and aboard the KC-135. I also wish to express sincere thanks to Dr. Ahmad Vakili and Dr. Roy Schulz for their advice and assistance as members of my review committee. Most of all I would like to thank my friends here at UTSI without whom I would not have been able to keep my sanity for so long.

ABSTRACT

The efforts reported in this thesis has been to analyze the data from two "Fluid Merging Viscosity Measurement" experiments in order to validate this as a viable method for measuring the viscosity of fluids with known surface tensions. This method involves simultaneously using a numerical analysis code and experimental data to produce matching curves of contact radius versus time and from that a determination of viscosity. Two experiments that were performed, used different liquids (glycerin and 125 Poise silicon oil) and different size ratios between the two drops (1 to 1 and 0.33 to 1 respectively). The experiments were performed aboard the KC-135 aircraft, "Weightless Wonder", and on the International Space Station. Both experiments produced accurate estimates of the viscosity for the experimental liquids. The glycerin viscosity fell within range of viscosity, which is dependent on temperature. The silicon oil viscosity was predicted to within 5% of its known viscosity value.

TABLE OF CONTENTS

CHAPTER 1: INTRODUCTION 1
CHAPTER 2: EXPERIMENTAL SETUPS 5
KC-135 EXPERIMENT 5
ISS EXPERIMENT 8
CHAPTER 3: MATHEMATICAL MODEL 13
TWO-DIMENSIONAL GEOMETRY 15
THREE-DIMENSIONAL GEOMETRY 19
CHAPTER 4: COMPUTER MODEL 23
EVOLUTION OF AN INITIALLY SQUARE SHAPE 24
INITIAL SURFACE GEOMETRY GENERATOR 24
EVOLUTION OF A MERGED DROPLET FROM TWO EQUAL DIAMETER DROPS 28
EVOLUTION OF A MERGED DROPLET FROM TWO INITIALLY DIFFERENT DIAMETER DROPLETS 30
CHAPTER 5: RESULTS AND DISCUSSION 39
KC-135 EXPERIMENT 40
DATA ANALYSIS 40
MODEL CURVE 42
VISCOSITY MEASURED 42
ISS EXPERIMENT 44
DATA ANALYSIS 44
MODEL CURVE 48
VISCOSITY MEASURED 48
AXIAL WIDTH 51
CHAPTER 6: CONCLUSIONS AND RECOMMENDATIONS FOR FUTURE WORK 57
REFERENCES 59
APPENDIX 63
APPENDIX A: NON-DIMENSIONAL ANALYSIS 64
APPENDIX B: INITIAL VALUE GENERATOR 66
VITA 69

LIST OF FIGURES

Figure ..... Page
1: Fluid Between Two Parallel Plates 1
2: Experimental Apparatus Flown aboard the KC-135 6
3: Frame of Actual Experiment Performed on board KC-135, where Two Glycerin Droplets are Brought Together to Initiate Merging. 7
4: Bridging Effect on KC-135 Experiment based on Two Initially Equal Sized Droplets 8
5: Experiment Apparatus Flown aboard the ISS 9
6: Frame of Actual Experiment Performed Aboard the ISS, Where Two Silicon Oil Droplets Are Brought Together to Initiate Merging 11
7: Two-Dimensional Cartesian Coordinate System 15
8: Shape Relaxation of Rounded Square with Time 25
9: Square Starting Values 26
10: Initial Value Circles 27
11: Equal Circle Initial Values 29
12: Equal Cylinder Progression until t* of 7.0 31
13: Non-Dimensional Contact Radius Progression with Time 32
14: Unequal Circle Initial Value 33
15: Progression of Unequal Cylinders with Time 34
16: Non-Dimensional Axial width Versus Non-Dimensional Time Step 36
17: Non-Dimensional Axial Width and Contact Radius Versus Non-Dimensional Time Step 37
18: Experimental Contact Radius Raw Data from KC-135Experiment for the Merging of Two Equal Diameter Drops 41
19: Model Contact Radius Variation with Time with Ratio of 1 to 1 43
20: Determining Time Scale by Matching Curves of the Growth of the Contact Radius of Two Initially Equal Droplets of Glycerin as the Droplets Merge with Sintering Computer Model for Cylinders with Radius Ratio of 1 to 1 45
21: Calibration Photos from ISS Experiment 46

22: Experimental Contact Radius Raw Data from ISS Experiment for the merging of Two Unequal Diameter Drops of Silicon Oil 47
23: Model Contact Radius Variation for Initial Droplet Diameter Ratio of 0.31 to 1 49
24: Comparison of Multiple Time Scales for the Growth of Contact Radius with the Experimental Merger of Two Drops of Unequal Diameter 50
25: Experimental Data on the Axial Width of Merging Droplet Pairs During Coalescence 52
26: Experimental Data on the Axial Width of Merging Droplet Pairs During Coalescence: Concentrated Time Axis with Local 2nd Degree Polynomial Curve Fit of the Data 53
27: Model Axial Width of Merging Droplet Pairs During Coalescence 54
28: Comparison of Multiple Time Scales on the Change of Axial Width with the Experimental Merger of Two Drops of Unequal Initial Diameter. 55

CHAPTER1: INTRODUCTION

Viscosity as defined by Young et al. (2001) describes the "fluidity" of a fluid. Comparing two liquids, they could have many of the same properties, such as density and specific weight, but they may flow completely differently due to the difference in their viscosity. To understand this property the example often given is Couette Flow, seen in Figure 1. This is flow between two parallel plates where the bottom plate is held firm while the top plate is moved. This top plate is pulled by a force acting parallel to the plate. For a given force, F, the speed at which the plate moves depends on its viscosity; the more viscous the fluid, the slower the plate moves.

In order to determine the viscosity of a fluid a device known as a viscometer is often used. Many different types of viscometers exist, ranging from very simple to complex devices, from counting the seconds for a liquid to drain off a stick to fully automated machines (Brookfield 2005). The dimensions of viscosity, in the general sense, are force·time per length squared (FTL^{-2}). In British Gravitational (BG) units viscosity is in $lb \cdot sec/ft^2$ and in the International System (SI) units it is $N \cdot s/m^2$. However, in here it will be described in the metric CGS (centimeter-gram-second) system with

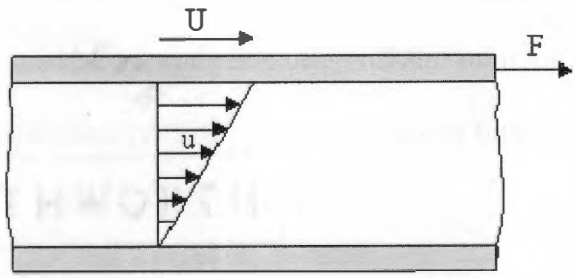


Figure 1. Fluid Between Two Parallel Plates.

units of g/cm·s which is referred to as a poise, P. The viscosity of water at room temperature is roughly 0.01 P or 1 centipoise (cp).

The other factor that plays a roll in the value of viscosity is the temperature of the material. The viscosity of gases increases with temperature, while in liquids the viscosity decreases with an increase in temperature (Pnueli 1992). This is due to the forces between molecules in a liquid decreasing with temperature. This relationship is often modeled in liquids allowing the viscosity to be determined solely by considering the temperature of the liquid. These models can be set up in order to accurately estimate the viscosity over a wide temperature range.

A major problem arises in trying to determine the viscosity of certain materials when it is impossible to obtain data at certain temperatures. For example, a metallic glass melt, PdSiCu, can be undercooled to a temperature of 575°c or 200 degrees below the melting temperature (Naka 1978).. Glass melts are said to be undercooled, which means that the melt is at a temperature below a phase transition temperature without the occurrence of the transformation (Callister 2000). At these undercooled temperatures, the liquid melt will crystallize with the introduction of a foreign object to act as a nucleation site; anything solid works adequately. Since all of the common viscometer instruments require the liquid to touch a solid boundary, undercooled liquids, such as low temperature glass melts, liquid metals, water etc., will crystallize and become solid when they touch the surface of a viscometer. When this happens it is impossible to obtain viscosity values at these temperatures and holes are left in the models which are usually presented graphically.

The only way to estimate the viscosity values of undercooled liquids is to

extrapolate from the liquid data that can be measured. These, however, has been known to greatly over and underestimate the true values (Etheridge et al. 1999). Many model equations exist to predict these values, but knowing which one is correct is impossible without having data points.

In order to determine the viscosity of these undercooled liquids, Antar et al. (2003) suggested a low-gravity containerless measurement technique. A terrestrial containerless technique - either by acoustic or magnetic levitation - will fail because of the sample deformation due to positioning errors, induced fluid circulation and gravitational body forces deforming the body shape. The proposed technique for this type of viscosity determination is based on both detailed measurements as well as numerical simulations of the shape relaxation properties of two merging liquid drops of the same liquid. The speed of evolution of the free surface and its geometry during the coalescence of two liquid volumes in a zero gravity environment is directly proportional to the liquid viscosity and its surface tension. It will be shown that by knowing the surface tension of the liquid, the viscosity can be determined by computing the rate of coalescence.

To avoid the problems associated with the terrestrial containerless techniques, a test bed with a long duration steady microgravity environment is needed. "Microgravity is a term commonly applied to a condition of free-fall within a gravitational field in which the weight of an object is reduced compared to its weight at rest on Earth" (Walls, 2005). Although we will always have a minute amount of gravity present, microgravity states allow other forces to dominate situations; for merging fluid droplets surface tension is the dominate force acting on the fluid. Test beds exist for simulating microgravity,

with approximate time of weightlessness of: drop tower (10 seconds), Parabolic flight aircraft (25 seconds), sounding rocket (1 minute), Space Shuttle (several days), and International Space Station (ISS) (months). A series of preliminary validation tests of the droplet merging approach to viscosity determination were done on board a KC-135 aircraft, in order to allow Antar et al. (1999) to monitor the process first hand. After the basic process was seen to be valid and practical, a more extensive experiment was planned that would take advantage of the long duration of microgravity aboard the ISS. Use of the steady test bed of the ISS eliminates a large "g-jitter" that was seen in the KC-135 experiments. It would also give the experiments much longer times to run, freeing up many constraints, allowing for a more open design of the experiment.

In the following sections of the thesis, the KC-135 and ISS experiments will be described. The theory that allows viscosity to be deduced from droplet geometry changes during merging will be discussed. The results from the KC-135 tests will be analyzed and the results and conclusions from these tests will be provided.

CHAPTER 2: EXPERIMENTAL SETUPS

KC-135 EXPERIMENT

A simple experiment was designed by Dr. Basil Antar and performed by Undergraduate students from the Texas Christian University on board of a NASA/KC-135 aircraft for the purpose of validating the drop coalescence method as a means for measuring the viscosity of liquids. The objective of the experiment was to allow two liquid drops to coalesce under the influence of only the surface tension force during a low-gravity segment of the flight parabola. A simple experimental platform capable of being carried on board the NASA KC-135 aircraft was designed to implement this objective. A sketch of the experimental configuration is shown in Figure 2, which includes a syringe pump, with two syringes, used for creating the liquid drops, the test cell within which the drops are made to coalesce, and a 16mm high speed movie camera for capturing the coalescence process. The test apparatus also included a tri-axial accelerometer with a digital readout. The test cell was fabricated from transparent Plexiglas® in the shape of a cube measuring 6.5cm on each side. Two 13-gauge hypodermic needles were attached on two opposite faces of the test cell, on whose tips the drops were formed. Each needle was connected to a separate hypodermic syringe, which were driven by the syringe pump. Different size syringes were used to allow the formation of different size drops. The precision syringe pump was capable of flow rates ranging from 1μl/min up to 100ml/min thus allowing the formation of a wide range of sizes for the drops. In this experiment glycerin was used to form the drops.

Each test was conducted by activating the syringe pump immediately after the low gravity segment of the flight parabola was attained. Once the drops reached their preset

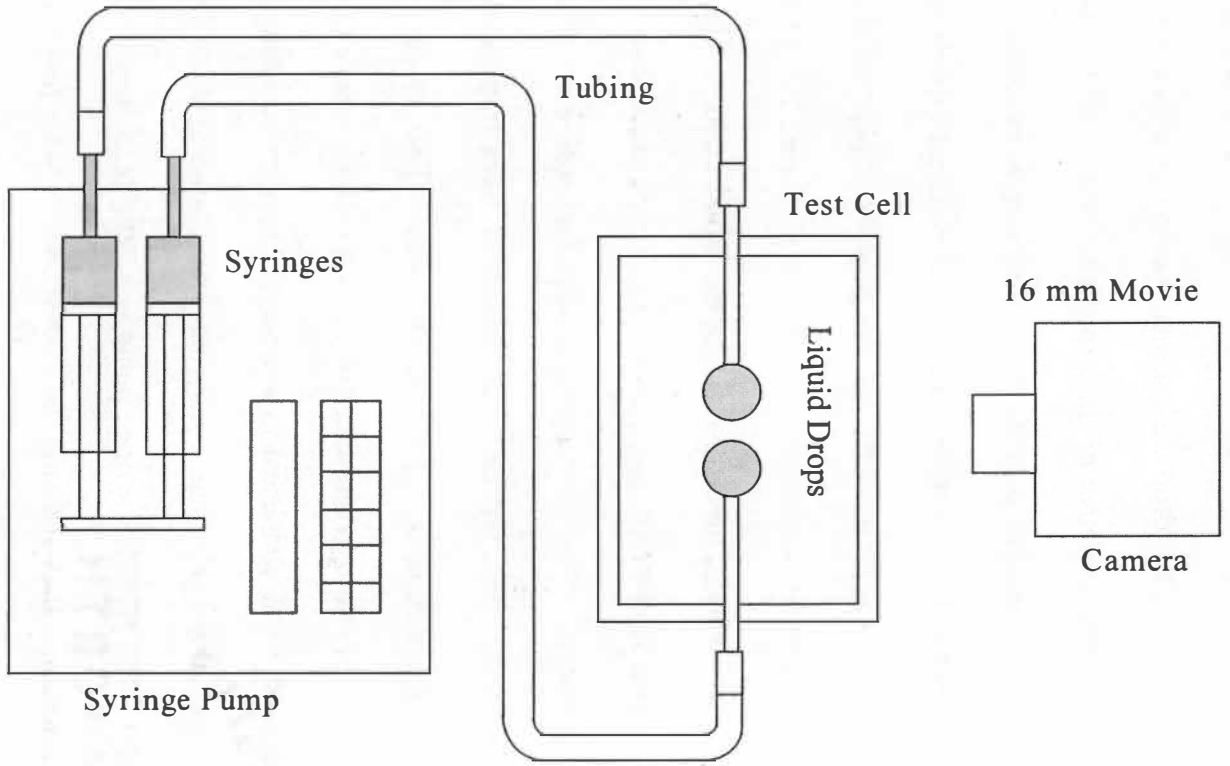


Figure 2. Experimental Apparatus Flown aboard the KC-135.

sizes, a low RPM motor will bring the drops together uniformly until they touch at which time the coalescence process was allowed to proceed independently under the influence of the surface tension force alone. The coalescence process was visually recorded using the high speed movie camera with frame rate of 500 frames per second; a frame from a typical recording is shown in Figure 3. The coalescence process was extremely fast for glycerin drops; normally achieved in less than 1 second. Tests were performed for different drop sizes ranging in diameter from 8 to 15mm, and for different fluids. However, the coalescence process was always performed with two drops of a single fluid. Measurements of the merging process were performed by analyzing sequences of

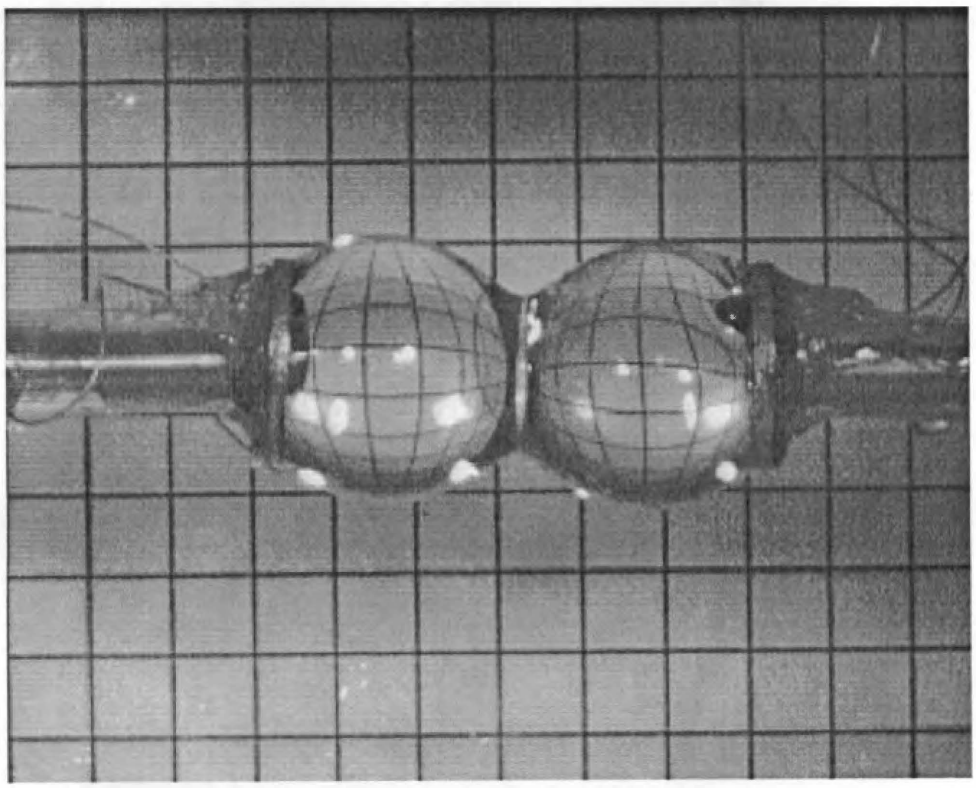


Figure 3. Frame of Actual Experiment Performed on board KC-135, where Two Glycerin Droplets are Brought Together to Initiate Merging.

individual film frames.

ISS EXPERIMENT

The validation experiment performed aboard the International Space Station (ISS) was performed by American Astronaut Mike Ficke. The objective of this experiment was the same as the one performed aboard the KC-135, to allow two liquid drops to coalesce under the influence of the surface tension force in a low gravity environment. Although the goals are the same, the setup was varied due to problems with the KC-135 experiment. The major problem was a bridging effect, seen in Figure 4, where at the end of the merging process data becomes ambiguous. Due to surface tension the drops do not separate from the syringes; they stay attached during the whole coalescence process. This means that the final shape is not that of a sphere, but more elliptical.

The experiment, sketched in Figure 5, was a very simple set-up with a low amount of payload sent up to the ISS. Restrictions dictated that only 1KG could be sent to the station, but any material already on board could be utilized. Upmassed materials included a background sheet with a known grid spacing of ½cm square and several

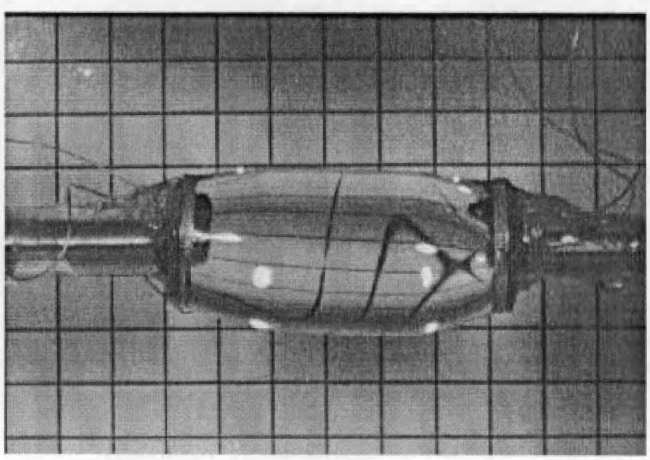


Figure 4. Bridging Effect on KC-135 Experiment based on Two Initially Equal Sized Droplets.

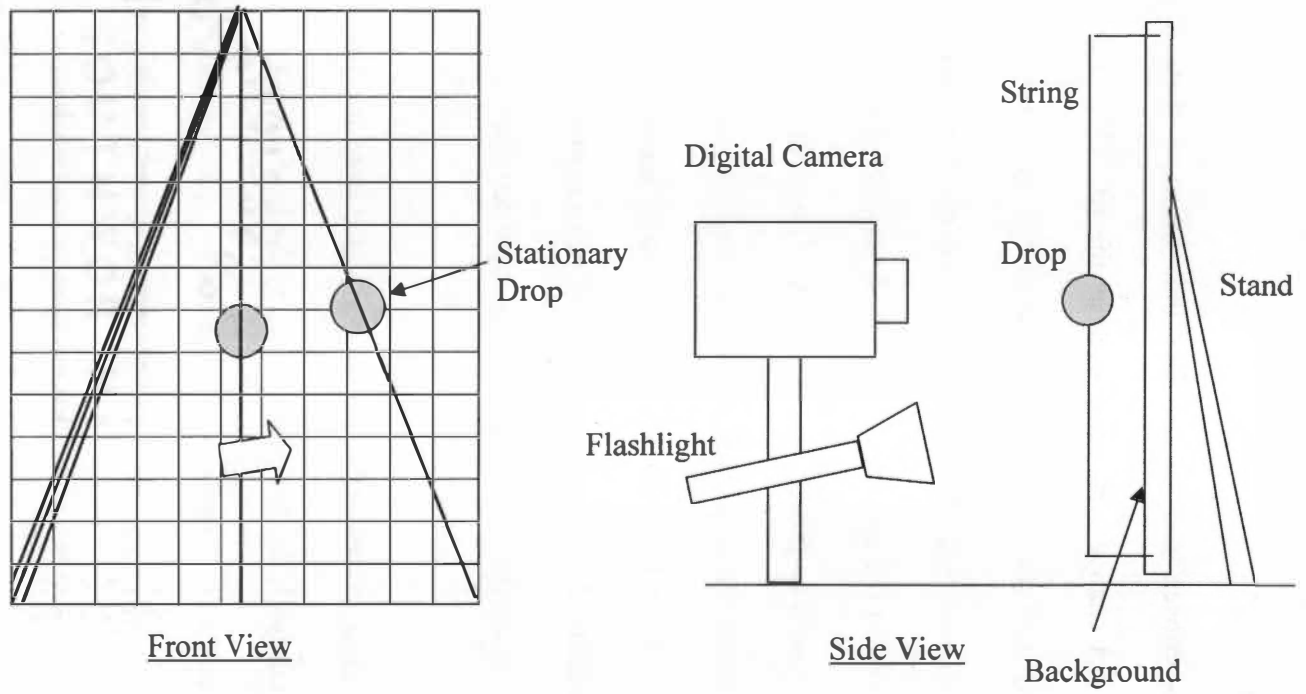


Figure 5. Experimental Apparatus Flown aboard the ISS.

syringes filled with various liquids. The background was attached to a stand that was already in orbit. Several strings, taken from a sewing kit on the station, were taped vertically in front of the background with a digital video camera and a flashlight pointed straight on to the strings.

This setup was chosen due to the fact that we now have a microgravity environment that does not change with time, such as the KC-135. The experiment is open to the environment and manually manipulated by the astronaut. The astronaut's first task was to separate one string from the group and inject a 1cc drop of liquid onto it. This string was then taped to the test stand. A second string was separated and another 1cc drop of the same liquid was placed on that string. These two strings were brought together in a slow manner so the drops would have little to no horizontal velocity as they touched. As soon as the drops were touching the tension on the incoming drop's string was released and coalescence due to surface tension alone took place. Once coalescence of the two spheres took place the two strings were brought together and anchored to the test stand.

A third string was separated and a 2cc drop injected onto it. This 2cc drop was then slowly brought to join with the 2cc drop created by the first merging. As soon as the two drops were made to touch, tension was again let off the incoming string and the surface tension caused the two drops to coalesce. All three strings were then combined and secured to the frame. A 4cc drop was then injected onto a fourth string. The two 4cc drops where then merged in the same manner as before. Finally a 0.5cc drop was injected onto the final string, slowly brought to the 8cc conglomeration and allowed to coalesce. Video tape of this sequence of coalescence process was then downloaded from

the ISS to NASA, placed on DVD and given to Dr. Antar and myself in digital format. Analyses were then performed on sequences of individual frames, similar to the one shown in Figure 6.

The ISS experiments were done with several different liquids of varying viscosities, to provide a wide range of measurements to apply the viscosity determination method. Two samples of silicon oil were used with different known viscosities. Glycerin of known viscosity and honey of unknown viscosity were also used. Honey is quite different from the rest of the liquids; it is a non Newtonian fluid meaning that its shear stress does not vary linearly with shear rate. Properties of the fluids used in the KC-135 and the ISS experiments are listed in Table 1.

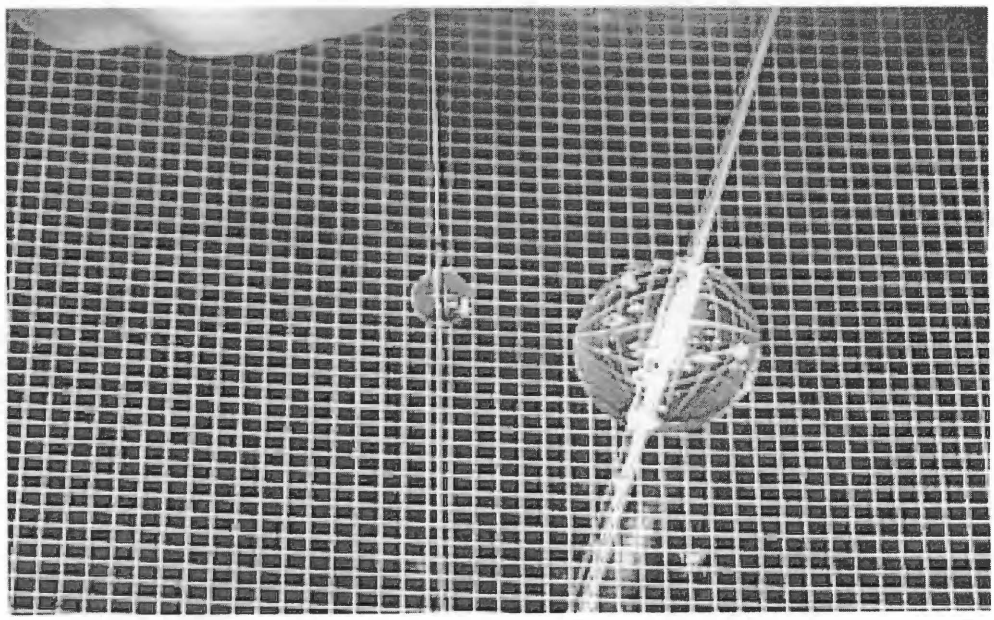


Figure 6. Frame of Actual Experiment Performed Aboard the ISS, Where Two Silicon Oil Droplets Are Brought Together to Initiate Merging.

Table 1. List of droplet properties for fluids used on the KC-135 and the ISS Experiments.

Liquid	Volume cc	Density g/cc	Surface tension Erg/cm^2	Viscosity Cp=mPa*sec	Variable within data set
Glycerin	1.0	1.17	63	1490	Temperature
	1.0	1.17	63	1170	Visc.=f(T)
	1.0	1.17	63	954	20 to 30 C
	1.0	1.17	63	629	
Silicone oil	0.5	0.97	21.5	12,500	
12,500cp	1.0	0.97	21.5	12,500	
	1.5	0.97	21.5	12,500	
	2.0	0.97	21.5	12,500	
Silicone oil	1.0	0.97	21.5	100,000	
100,000cp					
Honey	1.0	1.45	90	12,500	
	1.0	1.45	90	15,000	
	1.0	1.45	90	42,000	
	1.0	1.45	90	70,000	
	1.0	1.45	90	100,000	
Honey	1.0	1.47	88	42,000	
	1.0	1.47	88	54,000	
	1.0	1.47	88	70,000	
	1.0	1.47	88	100,000	
Corn syrup	1.0	1.41	83	2,200	
	1.0	1.41	83	15,000	

CHAPTER 3: MATHEMATICAL MODEL

An analytical formulation of the problem of liquid droplet coalescence can best be investigated with solutions of the equations of motion of an incompressible fluid. Throughout this chapter the analytical derivations followed that of Antar et al. (2003). They start by looking at the equations of conservation of mass and momentum of an incompressible fluid:

$$\vec{\nabla} \cdot \mathbf{u} = 0 \tag{1}$$

$$\frac{\partial \mathbf{u}}{\partial t} + \mathbf{u} \cdot \vec{\nabla}\mathbf{u} = -\frac{1}{\rho}\vec{\nabla}p + \nu\vec{\nabla}^2\mathbf{u} \tag{2}$$

where $\mathbf{u} = (u_1, u_2, u_3)$, is the velocity vector field, p is the pressure field inside the liquid mass, ρ is the fluid density, and ν is the liquid kinematic viscosity. Because we are interested in the merging of liquid drops under the influence of surface tension or capillary forces alone, the inertia terms can be neglected since the fluid motion is very slow which is a reasonable assumption for the coalescence problem. By neglecting the inertia terms the momentum equation becomes

$$\frac{\partial \mathbf{u}}{\partial t} + \mu\vec{\nabla}^2\mathbf{u} - \vec{\nabla}p = 0 \tag{3}$$

where μ is the liquid dynamic viscosity $(\mu = \rho\nu)$. Inertia terms are also eliminated in non-accelerating fluid motion such as Stokes Flow (Schlichting, 2001). Equation (1) and (3) are linear partial differential equations describing the viscous fluid motion for creeping flows which constitute the flows taking place in the coalescence of two liquid masses such as two liquid drops. Since the equations are linear, there exist closed form analytical solutions for this system in terms of the Stokeslets (Happel, 1965), depending

on the initial and boundary conditions.

The problem of sintering of materials is also basically concerned with the merging of two liquid masses. In the present project, we are interested in the free surface evolution as the masses merge. This makes the problem essentially a capillary one. Thus any solution to equations equation (1) and (3) must be consistent with the free surface boundary condition given by the following expression, representing the balance of surface forces:

$$\mathbf{T}\cdot\mathbf{n} = -\sigma\left(\frac{1}{R_1}+\frac{1}{R_2}\right)\mathbf{n} = \mathbf{b} \tag{4}$$

where **n** is the unit vector normal to the free surface pointing away from the liquids, σ is the coefficient of surface tension, R_1 and R_2 are the principal radii of curvature of the free surface, **b** is a surface tension vector, and **T** is the stress tensor which is given in Cartesian coordinates by its components

$$T_{ij} = -p\delta_{ij} + 2\mu\varepsilon_{ij}, \varepsilon_{ij} = \frac{1}{2}\left(\frac{\partial u_i}{\partial x_j}+\frac{\partial u_j}{\partial x_i}\right).$$

In order to create a representative mathematical model of the actual experiment, we need a three-dimensional model. However, in order to demonstrate the solution method adopted here in a clear manner and without the added geometrical complication of the spherical coordinate system, the solution method will be first outlined for a geometrically simpler rectangular Cartesian coordinate system. Below is an outline for the solution procedure for two-dimensional geometry representing the coalescence of two circular cylinders of infinite length.

TWO-DIMENSIONAL GEOMETRY

For the two-dimensional case of cylindrical drops, the set of governing equations (1, 3, and 4) for the liquid coalescence problem reduces to the following linear boundary-value problem for the velocity field with derivative boundary conditions, in a coordinate system shown in Figure 7:

$$\frac{\partial u_1}{\partial x_1} + \frac{\partial u_2}{\partial x_2} = 0 \tag{5}$$

$$\mu\left(\frac{\partial^2 u_1}{\partial x_1^2} + \frac{\partial^2 u_1}{\partial x_2^2}\right) - \frac{\partial p}{\partial x_1} = 0 \tag{6}$$

$$\mu\left(\frac{\partial^2 u_2}{\partial x_1^2} + \frac{\partial^2 u_2}{\partial x_2^2}\right) - \frac{\partial p}{\partial x_2} = 0 \tag{7}$$

$$p - 2\mu\left(\frac{\partial u_1}{\partial x_2} + \frac{\partial u_2}{\partial x_1}\right) = p_0 - \sigma\kappa \tag{8}$$

where κ is the curvature of the free surface given by $1/R$ for the two-dimensional case, and p_0 is the pressure of the air surrounding the liquid. Equations (5)-(8) are for steady state conditions in which the time dependence have been neglected. However, the time dependence of the solutions is obtained by marching the solution in time with time step

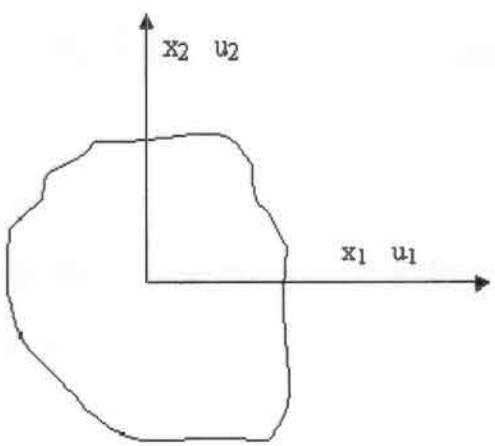


Figure 7. Two-Dimensional Cartesian Coordinate System

increments.

The region of flow is defined by a closed curve Γ and the interior area denoted by Ω. There exists a unique solution to the system (5) - (8) for the velocity field, $\mathbf{u}$, given in the following integral (see Antar et al., 2003):

$$c_{ij}u_j(x_i) + \int_{\Gamma} q_{ij}(x_i, y_i)u_j d\Gamma = \int_{\Gamma} s_{ij}(x_i, y_i)b_j d\Gamma \tag{9}$$

where in the above y is the position of a point on the surface Γ, while x is any point in the interior of the liquid mass Ω, (i = 1, 2) and (j = 1, 2) are the coordinate directions, and:

$$c_{ij} = \begin{cases} \delta_{ij} & \text{when } x \in \Omega; \\ \frac{1}{2}\delta_{ij} & \text{when } x \in \Gamma; ; \\ 0 & \text{when } x \in \Omega'; \end{cases}$$

$$q_{ij} = \frac{r_i r_j}{\pi R^4} r_k y_k$$

$$s_{ij} = \frac{1}{4\pi}\left[\frac{r_i r_j}{R^2} - \delta_{ij}\log R\right]$$

where $r_i = x_i - y_i$, $R = \sqrt{r_1^2 + r_2^2} = |x - y|$, δ_{ij} is the Kronecker delta, and Ω' is the complementary region given by $\Omega \cup \Gamma$. The solution given by (9) is in a non-dimensional form in which the velocity, pressure and time have scales with respect to the following velocity, pressure, and time scales respectively:

$$V_s = \sigma/\mu, \quad P_s = \sigma/L, \quad t_s = L\mu/\sigma \tag{10}$$

where L is an appropriate length scale, and for the geometry being considered in here could represent the radius of one of the cylinders. The non-dimensional analysis for these scales is presented in Appendix A.

Equation (9) can be written in the following vector symbolic notation:

$$C\mathbf{u}(\mathbf{x}) + \int_{\Gamma} Q(\mathbf{x},\mathbf{y})\mathbf{u}d\Gamma_y = \int_{\Gamma} S(\mathbf{x},\mathbf{y})\mathbf{b}d\Gamma_y \tag{11}$$

where C, Q, and S are the second rank tensors whose elements are c_{ij}, q_{ij} and s_{ij}, respectively. In order to ensure a unique solution to this problem equation (11) must be solved together with the added constraint that the liquid mass must be conserved at the free surface using the following mathematical representation:

$$\int_{\Gamma} \mathbf{u}d\Gamma = 0 \tag{12}$$

Equation (11) and (12) form the basic mathematical model for describing the coalescence process in a two-dimensional Cartesian system. Note that in this form the original differential equation system has been transformed to a system of bounded integral equations in which the free surface is represented by the integration bounds. Such integral formulation for the problem lends itself to a solution through an integral method such as a Finite Element Method (FEM) or the Boundary Element Method (BEM). The BEM is essentially a subset of FEM in which only the solution on the boundary of the domain, Γ, is sought while in the FEM the solution is obtained throughout the full domain, Ω, of the problem (Becker, 1992).

Equation (11) and (12) were solved using the BEM, a method that is ideally suitable for solving the boundary value problem for the free surface. Essentially, the BEM method performs the surface integrations given in (11) and (12) by subdividing the surface into segments. This is accomplished by allowing the surface boundary Γ to be discretized into a sequence of boundary curve elements (Γ_i), in which the velocity and surface tension force vectors are written in terms of their values at a sequence of nodal points in the following manner. After dividing the boundary Γ into N elements, Γ_1, Γ_2,..., Γ_N, we define velocity and surface tension force functions $\mathbf{u}$ and $\mathbf{b}$ which apply at

a typical element "j" in the following manner:

$$\mathbf{u} = \Phi u^j$$

$$\mathbf{b} = \Phi b^j$$

where u^j and b^j are the nodal element velocity and surface tension, respectively. The interpolation function Φ is a 2 x 2M matrix of shape functions which are the standard finite element-type functions given by

$$\mathbf{\Phi} = \begin{bmatrix} \phi_1 & 0 & \phi_2 & 0 & \cdots & \phi_M & 0 \\ 0 & \phi_1 & 0 & \phi_2 & \cdots & 0 & \phi_M \end{bmatrix} = \left[\Phi_1 \Phi_2 \ldots \Phi_M\right]$$

After substituting the shape functions into equation (11) and discretizing the boundary Γ we get the following expression for any arbitrary nodal point, i:

$$C^i u^i + \sum_{j=1}^{N} \left(\int_{\Gamma_i} \left(Q - Q^r\right) \Phi d\Gamma_\eta \right) u^j = \sum_{j=1}^{N} \left(\int_{\Gamma_i} \left(S - S^r\right) \Phi d\Gamma_\eta \right) b^j \tag{13}$$

Equation (13) can be written as a matrix equation in the following form by exchanging the summation and integration operators:

$$C^i u^i + \sum_{j=1}^{N} (F^{ij} - G_r^j) u^j = \sum_{j=1}^{N} \left(H^{ij} - I_r^j\right) b^j \tag{14}$$

where

$$F^{ij} = \int_{\Gamma_i} Q \Gamma d\Gamma_\eta; \qquad G_r^j = \int_{\Gamma_i} Q^r \Phi d\Gamma_\eta$$

$$H^{ij} = \int_{\Gamma_i} S \Phi d\Gamma_\eta; \qquad I_r^j = \int_{\Gamma_i} S^r \Phi d\Gamma_\eta$$

Equations (14) represent N algebraic equations for the N variables u^i, representing the velocity of the nodal points of the free surface curve, Γ. Solution of the system (14) yields the velocity of every nodal point. From knowledge of the velocity of every nodal point the shape evolution of the free surface curve can be determined as a function of

time by integrating the following equation at each time step, t:

$$\frac{d\mathbf{x}}{dt} = \mathbf{u}(\mathbf{x}) \tag{15}$$

Equation (15) gives us the time dependent shape of the free surface as the liquid drops merge. In the above solution method we begin with the initial geometry at time, t_0. This initial geometry is used to determine the velocity of the boundary after the first time step. From that velocity then the position x of the boundary can be determined by integrating $x_b = \int \mathbf{u} dt$. The new boundary is then used as initial conditions in the second time step and so on. This is called the time marching technique.

THREE-DIMENSIONAL GEOMETRY

In anticipation of the use of the numerical results in conjunction with experimental measurements, the coalescence of two dimensional circular cylinders is not exactly similar to the experiments which were performed with two spherical drops. Thus it is desired to express the mathematical model in terms of a three-dimensional method. However, since the drops do not very axially, meaning there is no change around the x-axis, we do not need a full three-dimensional spherical system. Due to this we can assume axial symmetry along the axis of merging giving $\frac{\partial}{\partial \theta} = 0$ as well as setting $u_\theta = 0$ with no swirl. With this is mind we can model the two spherical drops in cylindrical coordinates. To describe the previous analysis in these new terms we must transform the coordinate system thusly:

$$x_i = (x_1, x_2, x_3)^T = (r\cos\theta, r\sin\theta, z)^T \tag{16}$$

for the cylindrical coordinate system of (r, θ, z). Then the tensoral functions in (9),

namely c_{ij}, q_{ij} and u_{ij} must all be written for i,j=1,2,3 in the following manner:

$$c_{ij}\left\{=\delta_{ij},\ x\in\Omega;\quad =\delta_{ij}/2, x\in\Gamma;\quad =0, x\in\Omega'\right\} \tag{17}$$

$$q_{ij}(x_i,y_i)=\frac{3(x_i,y_i)(x_j,y_j)(x_k,y_k)n_k}{4\pi|\mathbf{x}-\mathbf{y}|^5} \tag{18}$$

$$s_{ij}(x_i,y_i)=\frac{1}{8\pi}\left[\frac{\delta_{ij}}{|\mathbf{x}-\mathbf{y}|}+\frac{(x_i-y_i)(x_j-y_j)}{|\mathbf{x}-\mathbf{y}|^3}\right] \tag{20}$$

Where again y represents a point on the free surface, while x represents an interior point.

After successive substitutions of the cylindrical coordinates in equation (7) and upon integration along the θ-direction, equation (7) takes the following form for cylindrical coordinates:

$$c_{\alpha\beta}u^c_\beta+\int_\Gamma q^c_{\alpha\beta}u^c_\beta d\Gamma=\int_\Gamma s^c_{\alpha\beta}b^c_\beta d\Gamma \tag{19}$$

Where the superscript c stands for cylindrical coordinates, and α and β are either 1 or 2 and hence $\mathrm{u}^c=\left(u^c_1,u^c_2\right)^T=\left(u_r,u_z\right)^T$. The coefficients $\mathrm{q}^c{}_{\alpha\beta}$ and $\mathrm{s}^c{}_{\alpha\beta}$ can be written in terms of complete elliptic integrals of the first and second kind (van de Vorst, 1995).

It can be seen from examining the governing equation (3) and the boundary condition (4) that the evolution of the free surface shape, as the two liquid volumes merge, is dependent upon the only two parameters that appear in these equations; μ and σ, the liquid viscosity and the surface tension coefficient, respectively. Also, due to the uniqueness of the solution of equation (13), the evolution of the free surface curve shape is also a unique function of the two parameters μ and σ, i.e.

$$\mathbf{x}=\mathbf{x}(t;\mathbf{x}_0,\mu,\sigma),\quad \mathbf{x}_0=\mathbf{x}(t=0)$$

In other words, the free surface shape evolution will be different for different values of either μ or σ. Thus, the objective of this analysis is to determine the viscosity of the liquid from the experimentally identified unique shape evolution of two merging liquid

volumes of the same fluid under the action of surface tension alone. This is accomplished by comparing the experimentally measured merging geometry and velocity of the free surface with the numerical approximation obtained from equation (13) together with the appropriate values for both the viscosity and surface tension.

CHAPTER 4: COMPUTER MODEL

An analytical solution to equation (9) was coded into a computer program as the numerical solution to the coalescence of the two drops; see Antar et al. (2003). This means that the computer model is setup for two-dimensional analysis. It is desired, however, to replace this with a three-dimensional form. Since the numerical method used to describe the system was a Boundary Element Method (BEM), only the free surface is of significance. Three programs have been constructed to assist in the modeling, the initial surface geometry generator, a double symmetry sintering program and a single symmetry sintering program. The sintering programs model the evolution of the free surface throughout the coalescence period until the system resolves to a shape of least energy, completely circular. To allow the computer program to be used for all materials, physical properties were replaced by non-dimensional variables, first seen in equation (10) of Chapter 3:

$$t^* = \frac{t}{t_s} \Rightarrow t = t^* t_s$$

$$l^* = \frac{l}{l_s} = \frac{l}{L} \Rightarrow l = Ll^*$$

where t* is the non-dimensional time, t is the physical time, t_s is the time scale, l* is the non-dimensional length, l is the physical length, l_s is the length scale. The time scale is then defined as $t_s = L\frac{\mu}{\sigma}$, where μ is the dynamic viscosity in units of $\frac{dyne \cdot s}{cm^2}$ and σ is the surface tension in units of $\frac{dyne \cdot s}{cm}$.

EVOLUTION OF AN INITIALLY SQUARE SHAPE

As a test of the program and for familiarization, the first shape that was analyzed as it evolved under surface tension was a square with rounded edges. Rounded edges prevent singularities from arising numerically in the program. As time progresses the square rounds out until it finally becomes fully circular, as seen in Figure 8. The program solution was done in time steps in increments of $0.01t^*$; however, the plot shows results at selected time steps to show surface geometry progression clearly.

The original program was set up based on double symmetry. That is the surface geometry in all four quadrants were symmetrical mirror images. This provided for easier input as only one quadrant needed to be defined, and the computer extrapolated the rest of the quadrants. For the double symmetry, only positive (x, y) values were entered into the program for the 1^{st} quadrant of the coordinate system. The initial values entered included all (x, y) pairs from the abscissa to the ordinate axes. For the square plot these coordinates can be seen in Figure 9, and numbered as $(x_{1,1}, x_{2,1})$ to $(x_{1,n}, x_{2,n})$.

INITIAL SURFACE GEOMETRY GENERATOR

In order to organize equally spaced data points for the boundary surfaces of two merging circles, an initial surface geometry generator program was created. The program displays coordinate points after the user specifies the total number of data points to be used, the radius of the two circles, and the initial contact radius. A schematic of the problem requiring the generator program is presented in Figure 10. After the size of the cylinders and the initial contact radius has been entered, the program measures the angles from the contact radius to the x-axis on both circles. The number of data points is then divided proportionally between the two circles.

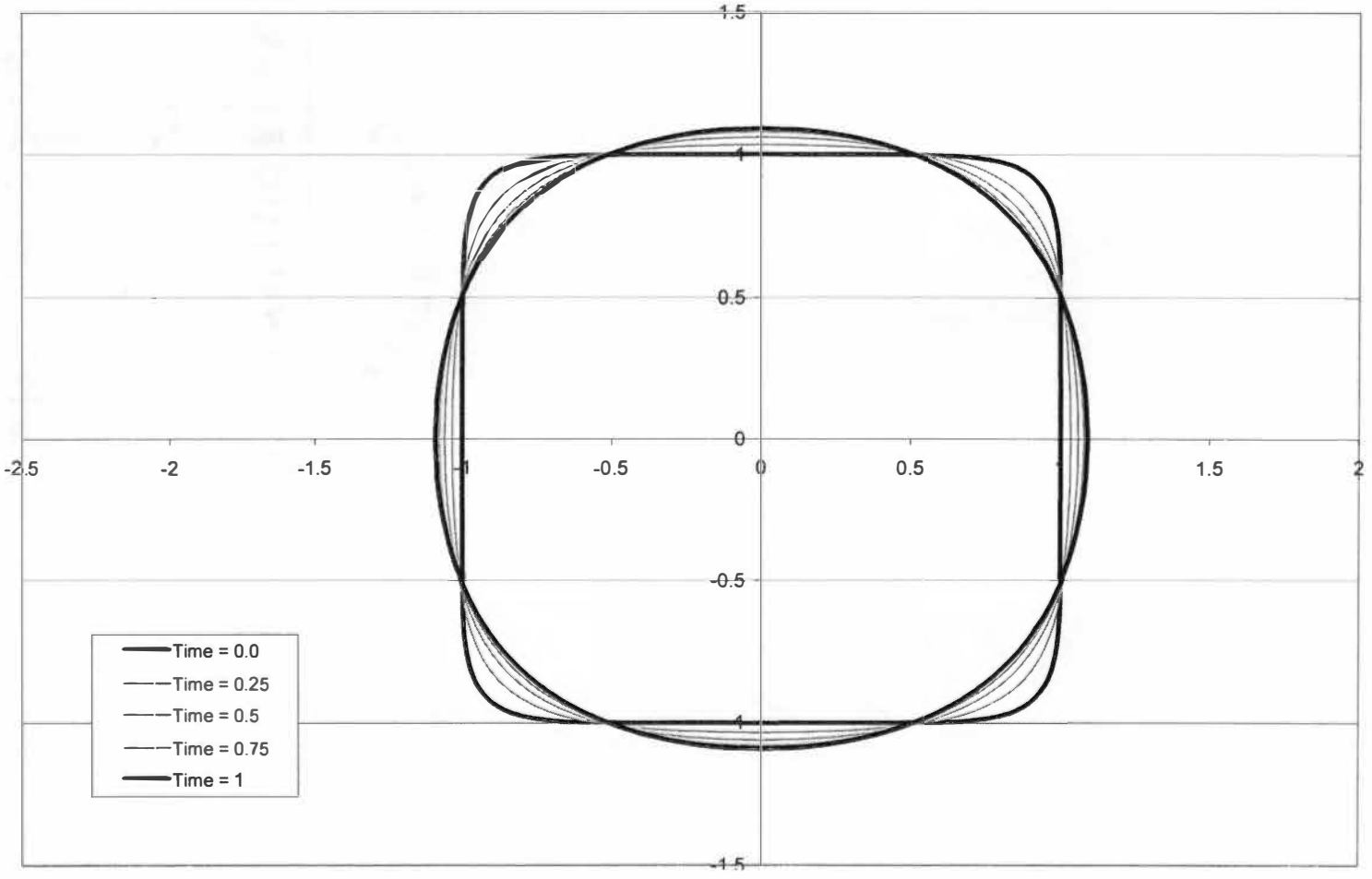


Figure 8. Shape Relaxation of Rounded Square with Time.

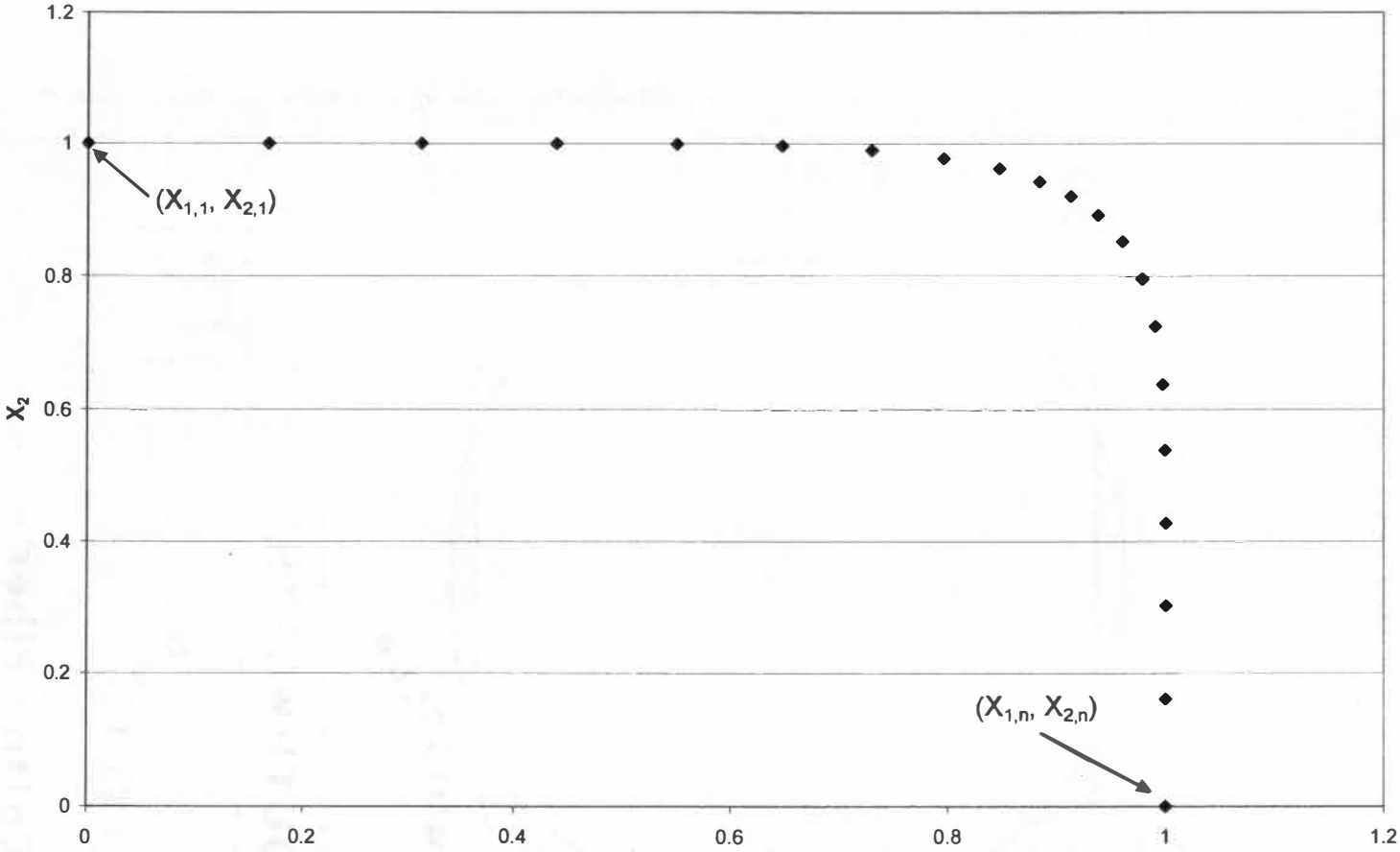


Figure 9. Square Starting Values.

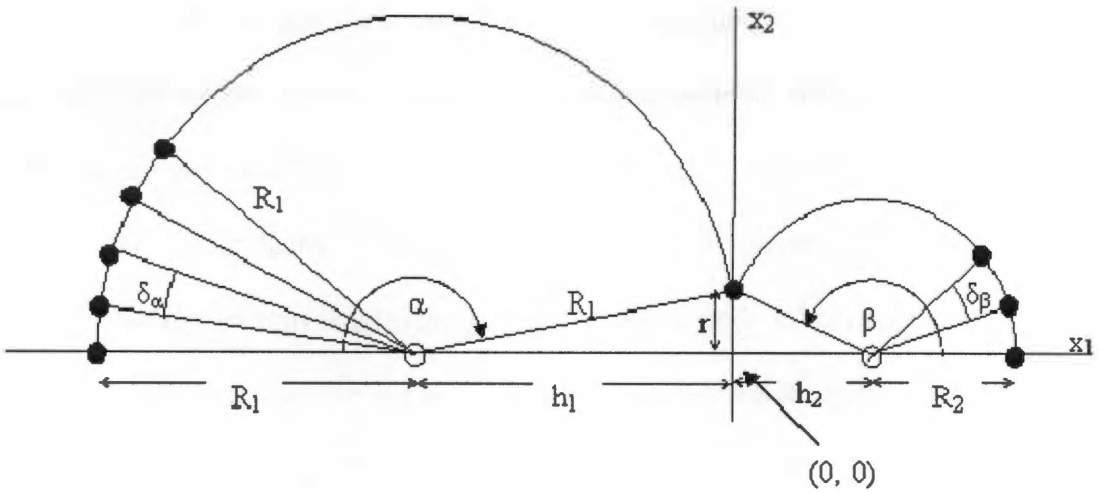


Figure 10. Initial Value Circles

The focal point of the left circle is placed a distance of h_1 away from the origin, which is calculated as $\sqrt{R_1^2 - r^2}$, where R_1 is the radius of the left circle and r is the initial contact radius between the two circles. The first value of the coordinate (x_1, 0) or the first point, is at $x_1=-(h_1+R_1)$ and $x_2=0$. The following points are located at $x_1=-(h_1+R_1\cos(c\cdot\delta_\alpha))$ and $x_2=(R_1\sin(c\cdot\delta_\alpha))$, where c ranges from 0 to n_1, the number of points in the left circle. This continues until x_1 is equal to 0, which occurs at $x_2=r$. Plotting then is transferred to the right circle with its focus at (h_2,0), where h_2 is similarly calculated as $\sqrt{R_2^2 - r^2}$. Points are plotted here at $x_1=(h_2+R_2\cos((n_2-c)\cdot\delta_\beta))$ and $x_2=(R_2\sin((n_2-c)\cdot\delta_\beta))$, where n_2 is the total number of points in the right circle and c goes from 1 to n_2. This continues until the last point is reached at $x_2=0$ and $x_1=h_2+R_2$.

The generator outputs these points into a text file, which can be opened as is or imported by Excel®. A graph of these points is then created to ensure a proper boundary. Once certain that these points are correct, the desired portion of the circles are taken and placed into a sintering program.

The initial geometry generator discussed above does not take into account the volume change due to the merging process. It only sets up two circles of finite radii without coalescence. A better initial geometry estimator would be to use the analytical solution developed by Frenkel for two merging spheres of equal radii. The Frenkel solution is quite accurate for short times up to non-dimensional time of 1 (Pokluda et al., 1997). For longer times the Frenkel analytical solution has been extended by Pokluda et al. (1997). However for the case of two circular cylinders the solution of Hopper (1984) can be used for initial short times.

It should also be noted that the contact radius used in the computer model has a finite value at time $t^*=0$. This was necessary due to the fact that severe numerical difficulties may be encountered if the numerical computations were initiated at the precise time of contact for which case the contact radius is zero in both cases. To avoid such difficulties the computations were always initiated at a finite, but small, value for the contact radius. The smallest contact radius possible in the present computations was of the order $\ell^*(t^*=0)\approx 0.1$. It should be noted that this approach does not introduce errors in the solution whenever it is properly handled.

EVOLUTION OF A MERGED DROPLET FROM TWO EQUAL DIAMETER DROPS

With equal sized drops double symmetry still is in use. This means that only the right semicircle of the initial surface geometry needs to be entered. In Figure 11 the initial values for the cylinders are shown as diamonds and the computer added points are shown as "-" marks. The code predicted the merging of the two cylinders to coalesce, after a given number of time steps. At each time step, updated values of the free surface

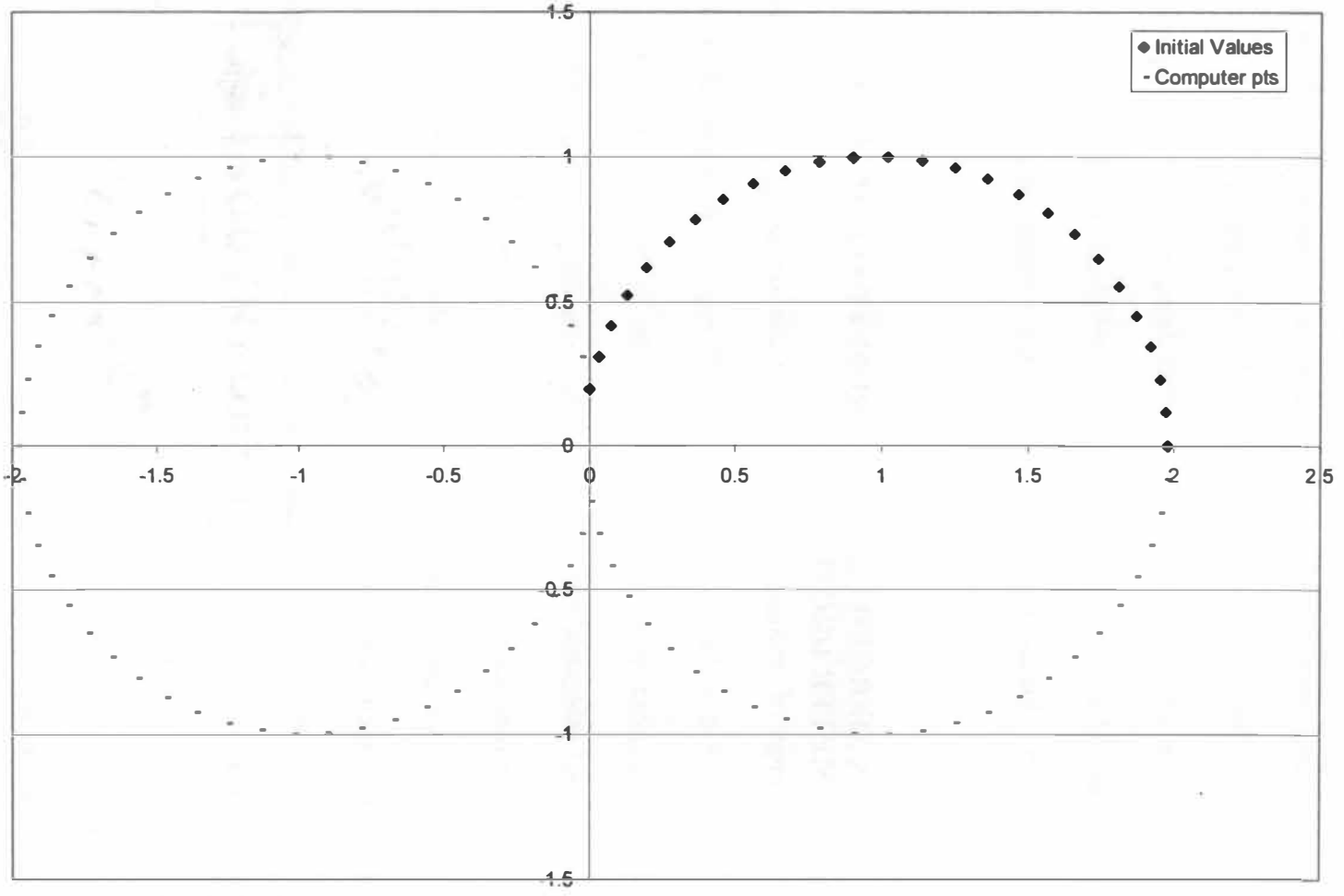


Figure 11. Equal Circle Initial Values.

are given, as seen in Figure 12. Although we have the entire free surface at each time step, only one value is of major importance in determining the surface tension. That value is the contact radius, or size of the neck area between the two circles. Comparing the contact radius size versus time between what the computer model predicts to experimental data is how viscosity is calculated. A separate output file was set up solely containing the contact radius at each time step. For equal sized circles this point was always located at x_1=0. Figure 13 shows a plot of the contact radius size as time progresses.

EVOLUTION OF A MERGED DROPLET FROM TWO INITAIALLY DIFFERENT DIAMETER DROPLETS

To explore drops of unequal diameter we use the single symmetry sintering program. Free surface points of positive x_2 values are only entered into the program; then the program creates the negative x_2 side of the graph. This is shown in Figure 14 with diamonds as the entered values and the "-" marks as the computer generated points.

However, determination of the contact radius of initially unequal diameters of cylinders presented a problem because the x_1-value of the contact region migrated towards the side of the smaller drop, as seen in Figure 15. And after the contact surface no longer has a discernible dip, the measurement of the contact radius is ambiguous. This does not mean that we cannot use the contact radius in this case; we just will not get a complete set of data. In order to create a curve that was continuous over the entire coalescence process, the total distance between the two farthest points on the abscissa were taken. These are the axial points where both lay on $x_2 = 0$. An output file similar to the contact radius for the equal circles was created here displaying the time step and the

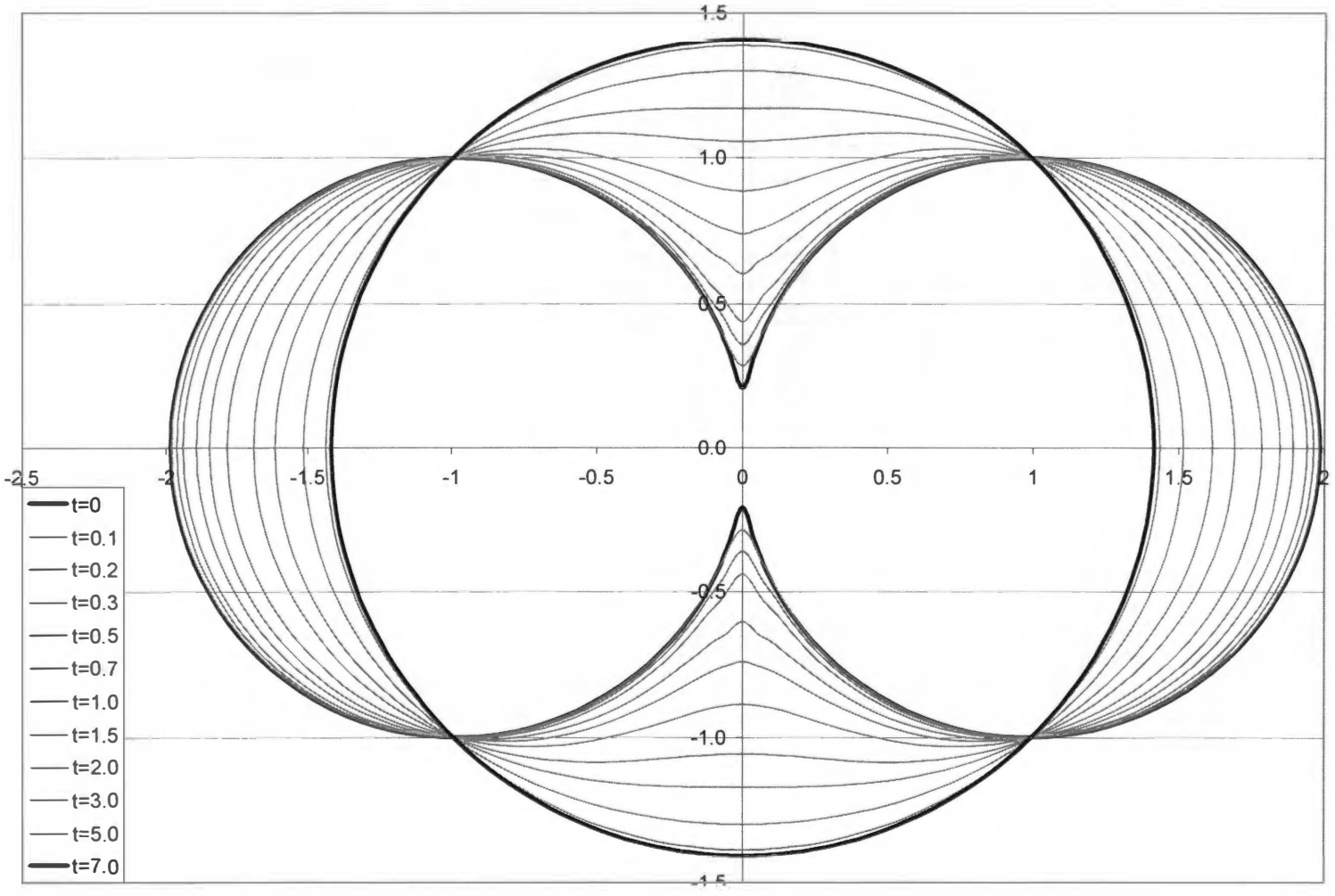


Figure 12. Equal Cylinder Progression until t* of 7.0

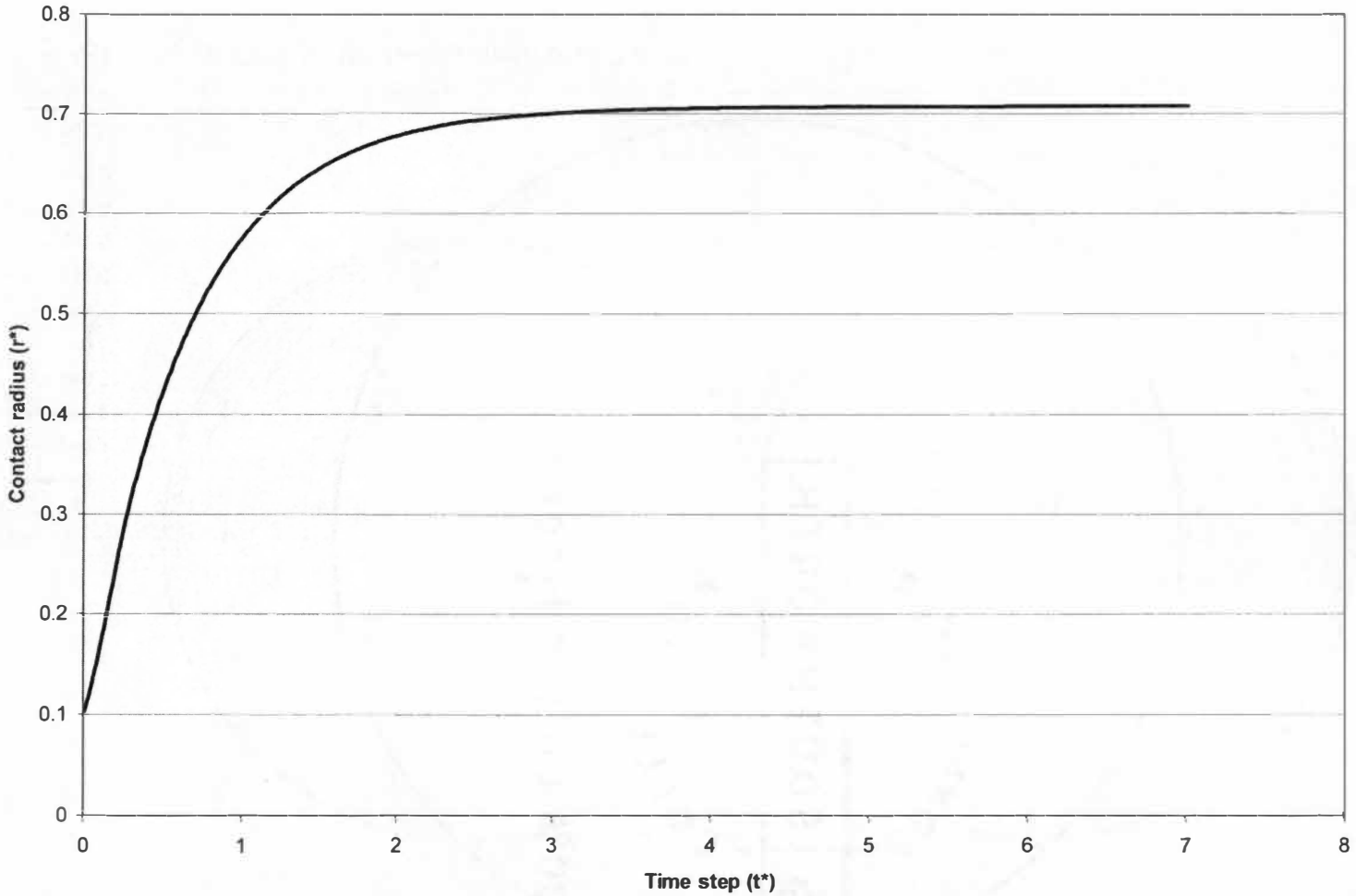


Figure 13. Non-Dimensional Contact Radius Progression with Time.

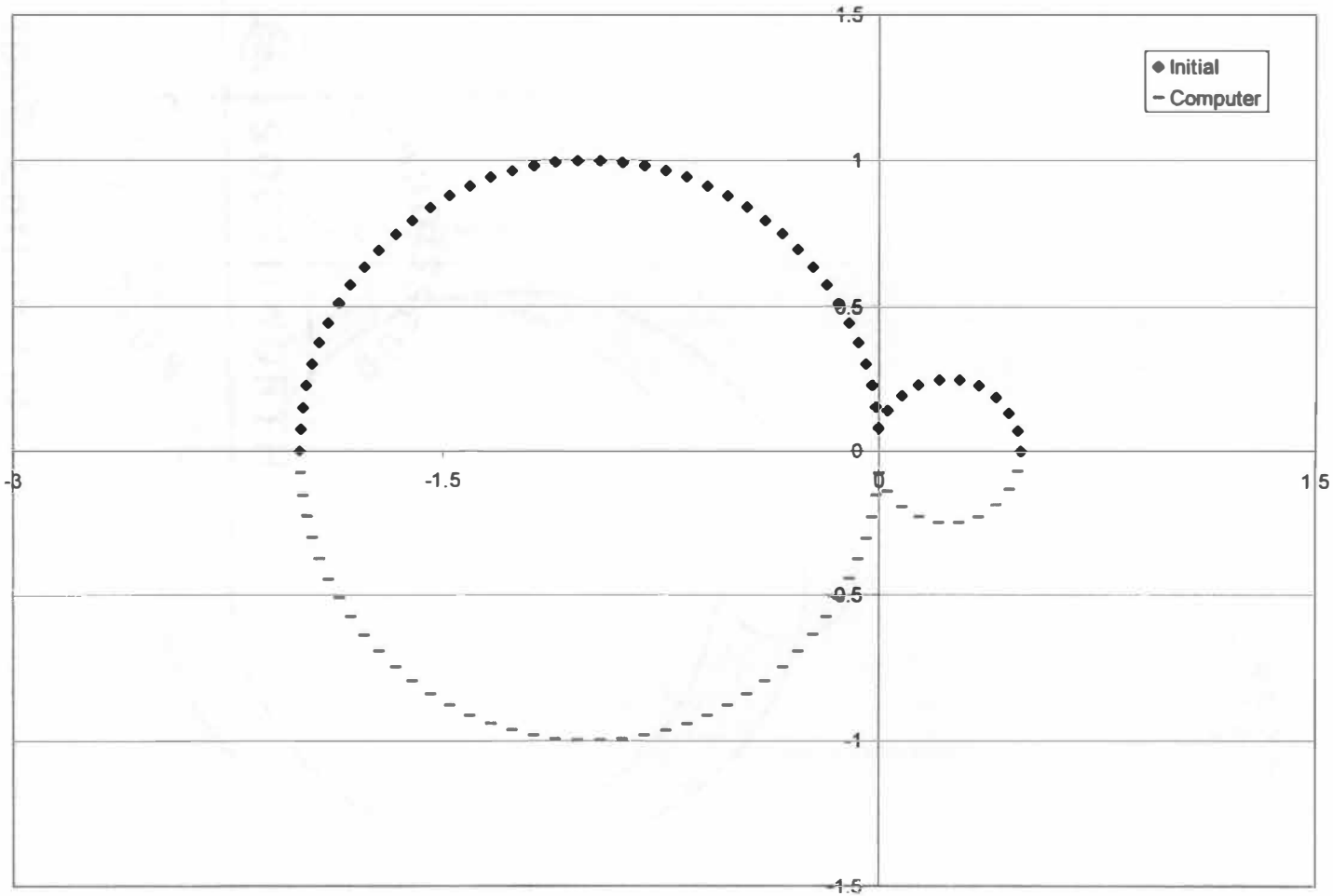


Figure 14. Unequal Circles Initial Values.

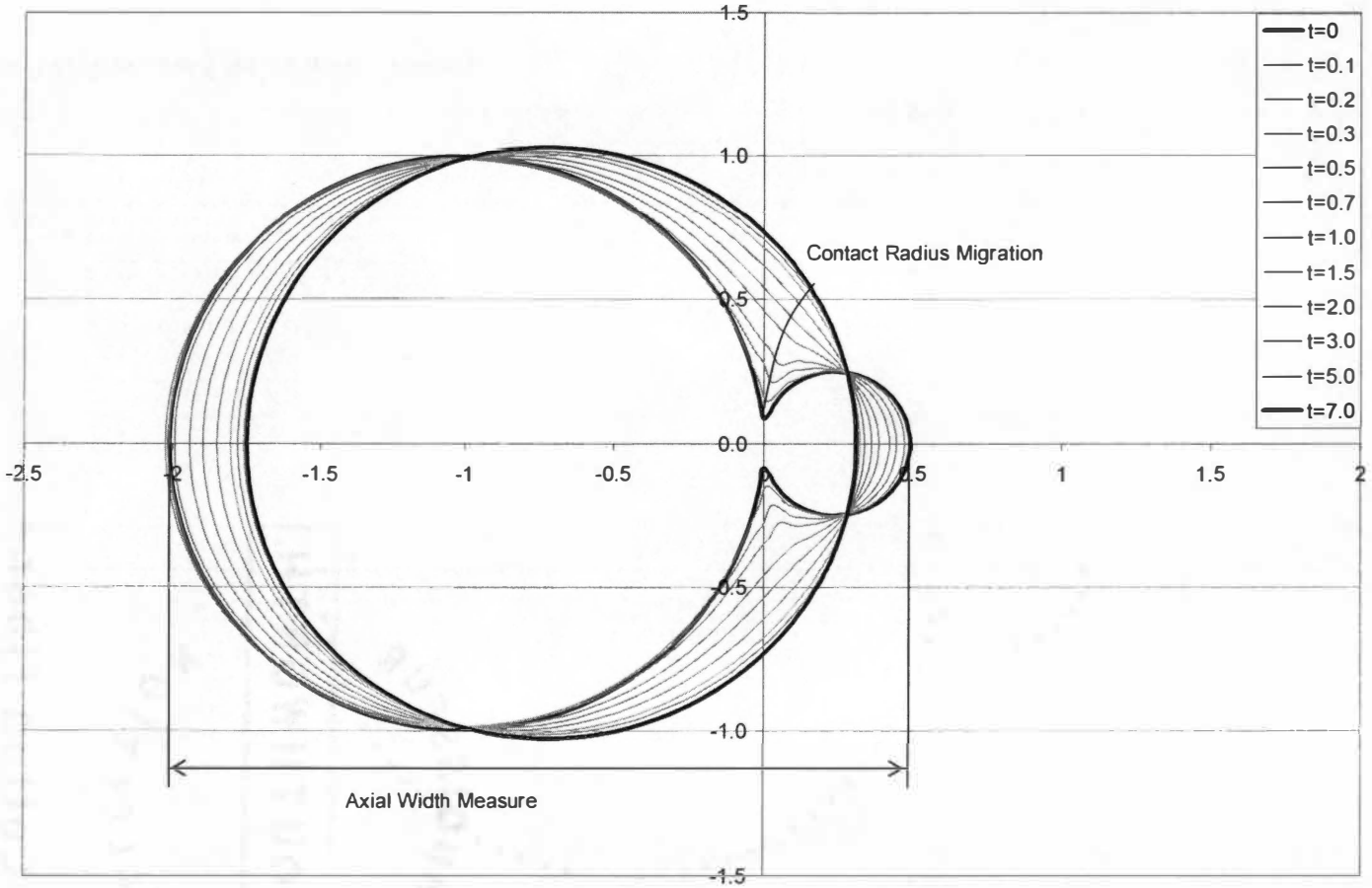


Figure 15. Progression of Unequal Cylinders with Time.

two x_1 values at each $x_2 = 0$ point. The distances are plotted versus time in Figure 16. Figure 17 is a combination of the non-dimensional contact radius and the axial width, both versus the non-dimensional time step t^*. This shows how much more data can be collected when looking at that axial width instead of the contact radius.

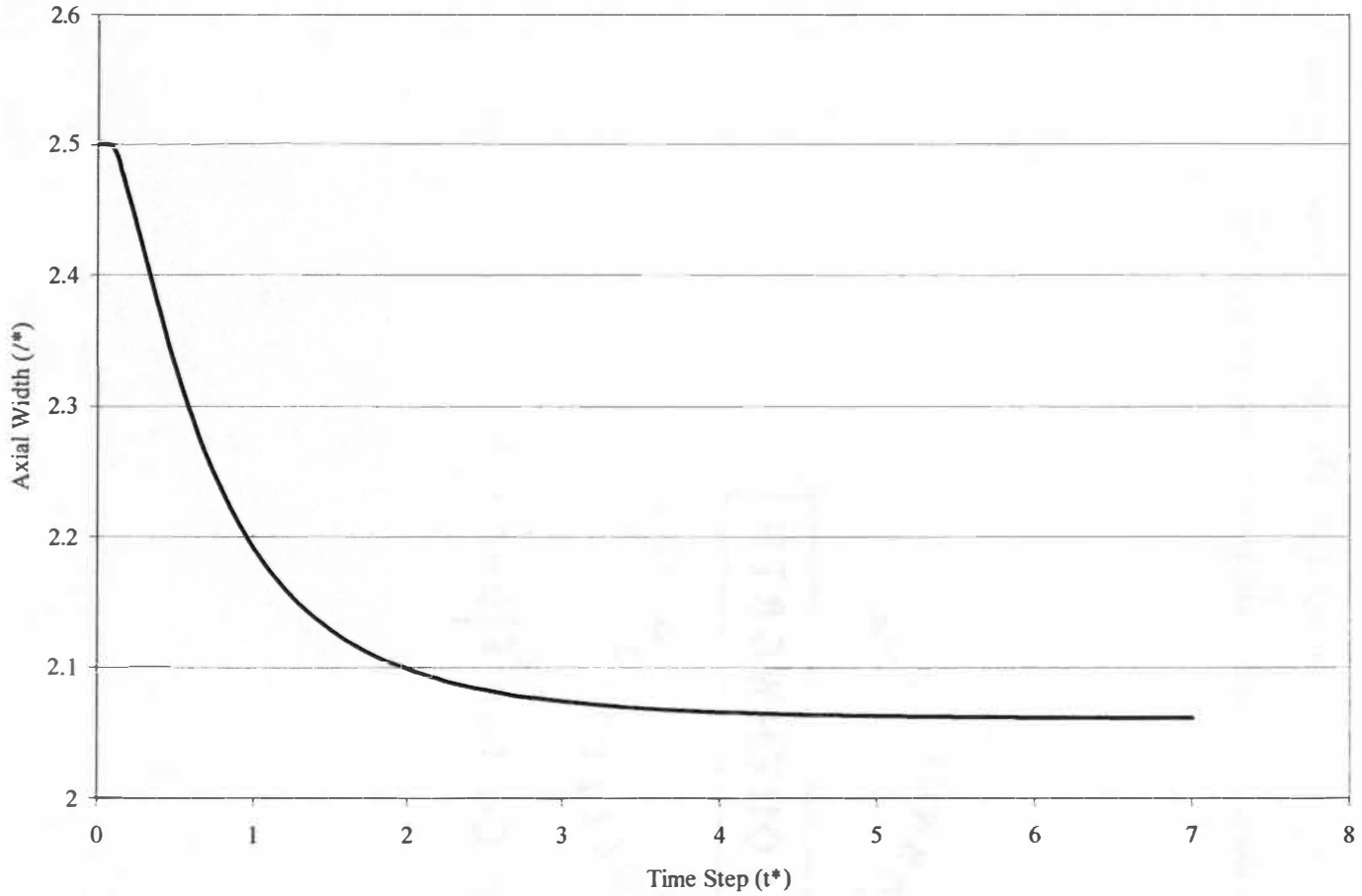


Figure 16. Non-Dimensional Axial width Versus Non-Dimensional Time Step.

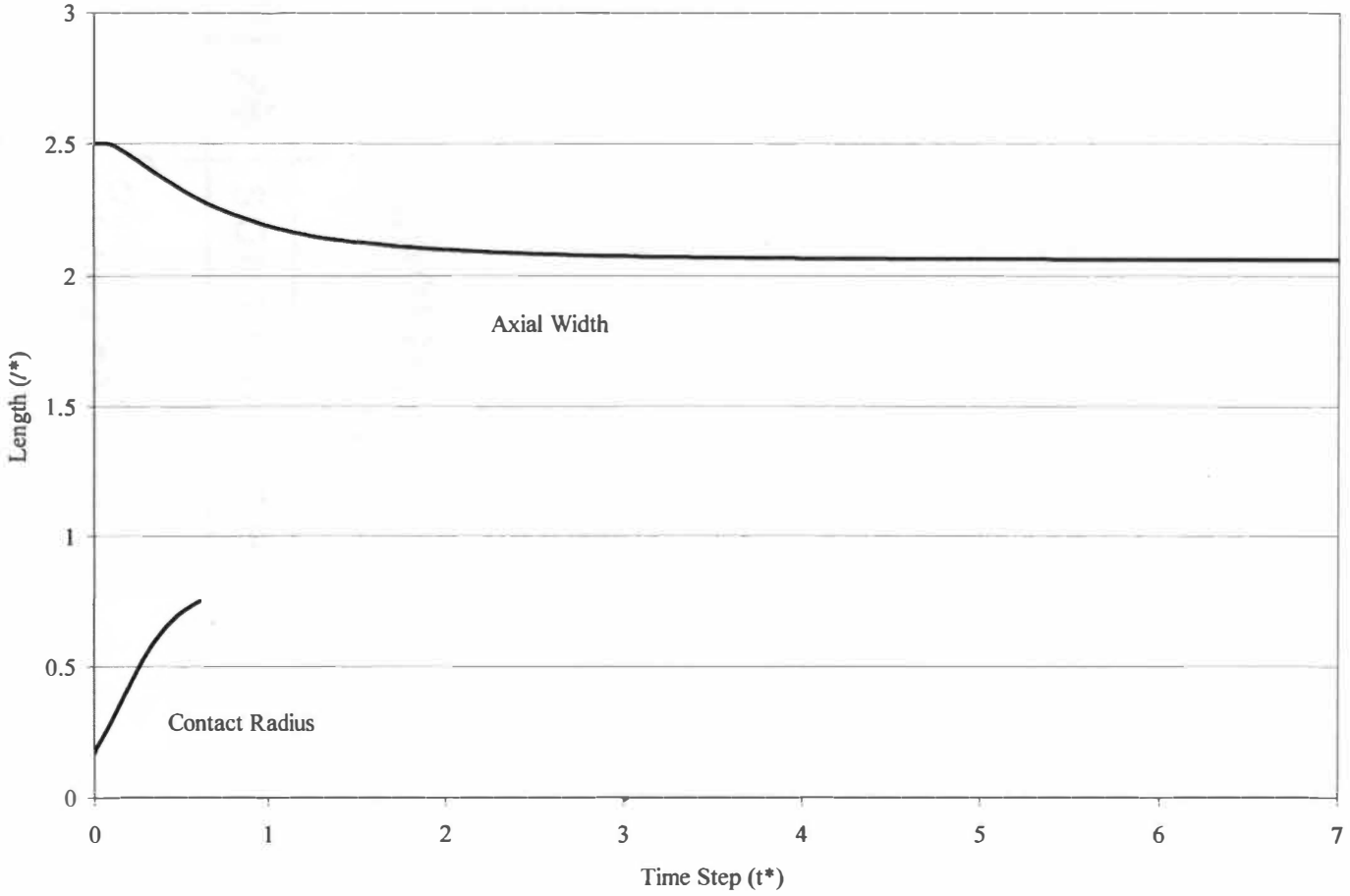


Figure 17. Non-Dimensional Axial Width and Contact Radius Versus Non-Dimensional Time Step.

CHAPTER 5: RESULTS AND DISCUSSION

A series of trials were performed aboard both the KC-135 and the ISS with various liquids. However, for this thesis, only one sequence from each was analyzed. The main data source was videos taken during each experiment. The video from the ISS experiment was delivered on DVD in a VOB format, which is a multiplex of video and audio data. Before any analysis could be performed, this video needed to be separated into individual frames. To do this the files were converted to an Audio Video Interleave (AVI) format, the most common file format for storing audio/video data on the PC, to allow for an AVI splitter to break the video into its individual frames. The AVI converter also gave information about the videos, the KC-135 video had a resolution of 320x280 and the ISS video's resolution was 740x480.

Once the videos had been broken into their frames, a NASA program called Spotlight™ was used to take length measurements of the images. Spotlight was written to analyze sequences of images generated in fluid physics experiments (Klimek, 2004). It is specifically designed to track points over a sequence of frames. By specifying areas of interest (AOIs), a user can manipulate a frame in order to more accurately find certain points. These points are either tracked manually by clicking on them with the mouse, or automatically by varying contrast or another distinguishing marker.

To ensure that accurate data points were established, manual AOI tracking was used. This required the user to click on a point to be measured and then the program centers the AOI on that point. Two AOIs were used in each series of data analyses. For experiments with equal sized drops, the AOIs were placed around each of the contact

cusps, which are the dips where the two drops meet, i.e. at the contact radius. For experiments that studied the merging of unequal sized drops, one analysis was done similar to the equal drops, while another analysis based on placing the two AOIs on the far edges of the two drops, to measure the full length of the two drop system. This program, however, only gives distances in terms of pixels. The full number of pixels in the KC-135 images stayed the same, where for the ISS images the resolution was cut in half on Spotlight™ to 360x240 pixels.

KC-135 EXPERIMENT

DATA ANALYSIS

Data was taken from a Spotlight™ text file and entered into Excel® where it was manipulated to present physical data. To convert number of pixels into a meaningful measure of length, a calibration was performed. The experiment had a background with grid spacing of ½cm behind the merging drops. Spotlight™ was used to measure the length of these squares, which averaged to 27 pixels. A column in the Excel® data sheet was then included to convert the number of pixels in the KC-135 data into centimeters by dividing the data by the 54 pixels/cm calibration number that was determined.

The lengths then need to be plotted versus time to produce any truly meaningful data. From Spotlight™ we tracked certain points in every frame that we created from the video files. From the film speed of the camera we calculated the time between each frame in the video. Dividing each frame by the frame speed gave the approximate time of that data point: $\frac{\text{No. frame}}{500\ \text{frames}/\text{sec}} = \text{sec}$. Figure 18 shows the contact radius raw data in engineering units, of cm versus seconds, for the experiment based on merging equal

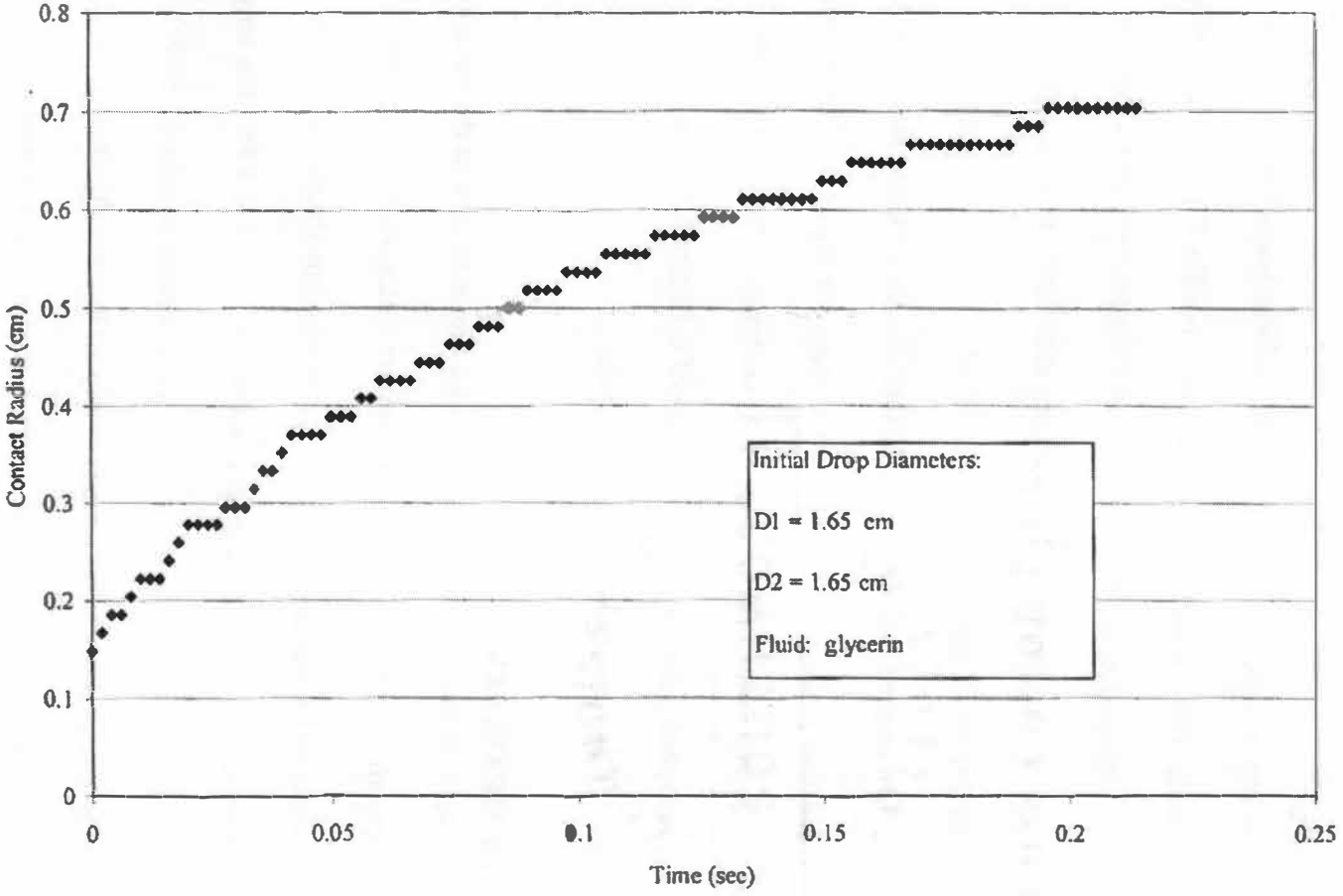


Figure 18. Experimental Contact Radius Raw Data from KC-135Experiment for the Merging of Two Equal Diameter Drops.

drops of the KC-135 flight. Note that the first data point recorded had a contact radius of 0.15 cm and not 0 length. We were not able to observe the r=0 data from the video.

MODEL CURVE

The next step taken in determining the viscosity of the liquids was to create a computer model for the size ratios found in the experiment. For the KC-135 experiment we know the drops are of equal size, so in the model each cylinder will have a radius of 1 ℓ^* creating a ratio of 1 to 1. In Chapter 4 the computer generated curves are plotted in non-dimensional length (ℓ^*) versus non-dimensional time (t^*).

This ratio was then entered into the Initial Surface Geometry Generator to obtain the initial geometry that was placed into the sintering computer program. This provided the non-dimensional equivalent for the drops we were analyzing. The contact radiuses versus time were then graphed using Excel® and presented in Figure 19. This figure is in non-dimensional form, which is changed in the next section.

VISCOSITY MEASURED

Since the viscosity is buried in the time scale, we dimensionalized the computer model and matched it with the data curve to find the correct scales and the viscosity. The length was the first thing to be changed, done by multiplying our length scale to the ℓ^* value. This is very simple since we set the radius of the large circle to 1 ℓ^*. The length scale then was the radius of the large drop before coalescence, measured earlier by Spotlight™. A column in Excel® was set up to multiply all the non-dimensional lengths by this scale. For the equal-sized drops, the value of the length scale was 0.83 cm.

The next issue was to transform the non-dimensional time, t^*, into a time, t, in

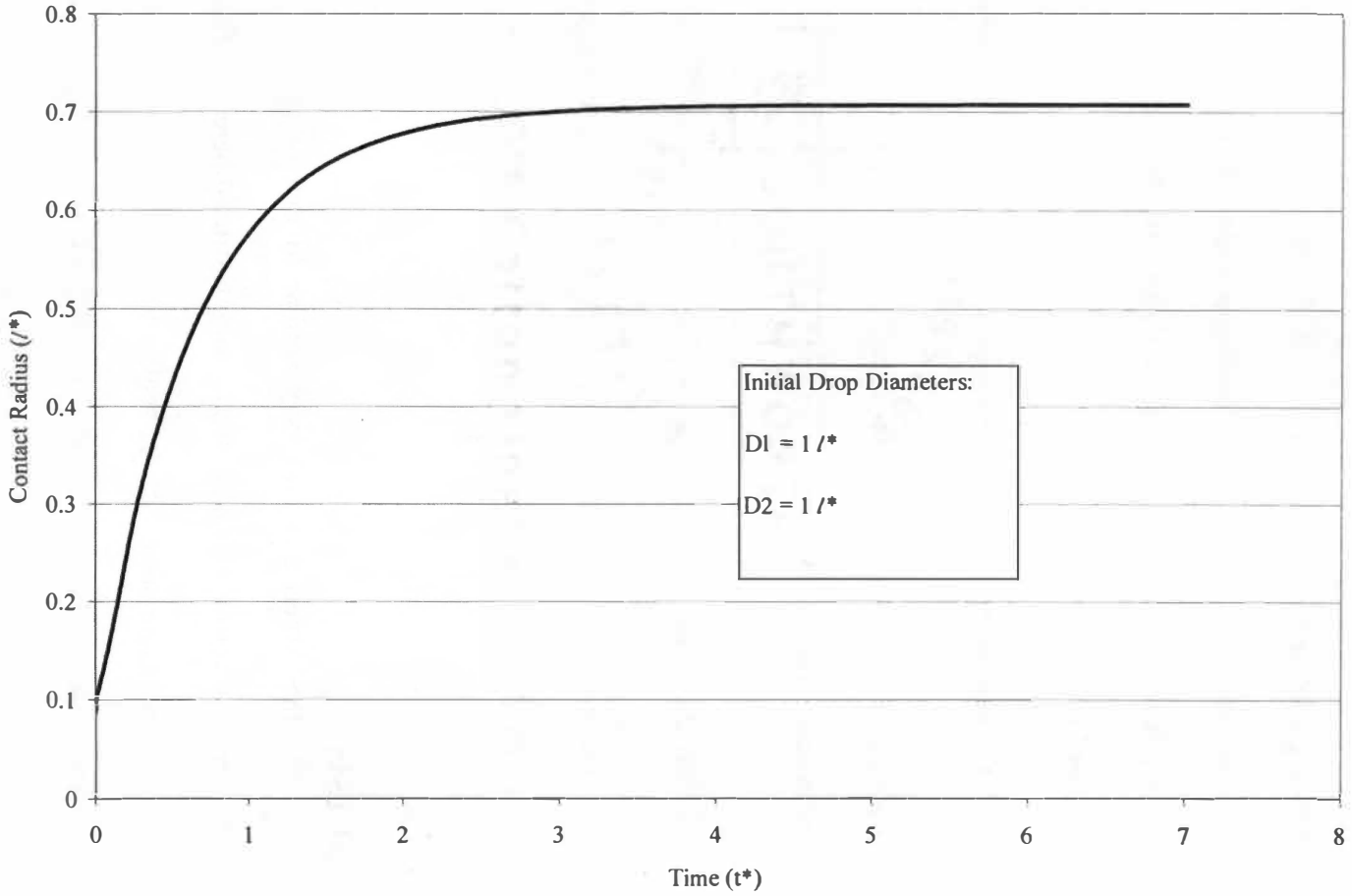


Figure 19. Model Contact Radius Variation with Time with Ratio of 1 to 1.

seconds. However, since the time scale, t_s, is defined by the viscosity that we are trying to determine: $t_s = \frac{r_s \cdot \mu}{\sigma}$, we cannot simply calculate its value. To determine the time scale we implemented a guess and check technique. With the two curves plotted together, the physical data is held constant, the length scale is already determined and we varied the time scale. A cell was set up in Excel® which allowed the time scale to vary until the two curves matched up, as in Figure 20.

Once the value of t_s was found, we put it into the equation $\mu = \frac{t_s \cdot \sigma}{l_s}$ to obtain the viscosity. The time scale for the equal drops of the KC-135 experiment is 0.17 seconds. With the length scales from above of 0.83 cm and the known surface tension of 63 dyne/cm for the glycerin, the equation above becomes $\mu = \frac{0.17\,\text{sec} \cdot 63\,{}^{\text{dyne}}/_{\text{cm}}}{0.83\text{cm}}$ which equals 12.9 dyne·s/cm. The nominal value of viscosity for glycerin varies between 6.3 dyne·s/cm and 14.9 dyne·s/cm depending on the temperature of the liquid.

ISS EXPERIMENT

DATA ANALYSIS

The analysis of the ISS experiment was very similar to that of the KC-135 experiment. Although a grid background with known spacing was used here as well, we did not need to rely on that for a calibration. At the beginning of the ISS experiments, a special calibration sequence was performed. A ruler, marked off in 1cm lengths, was placed both horizontally and vertically into the visual background, seen in Figure 21. Spotlight™ was then used to measure the length of the tick marks in pixels. An average

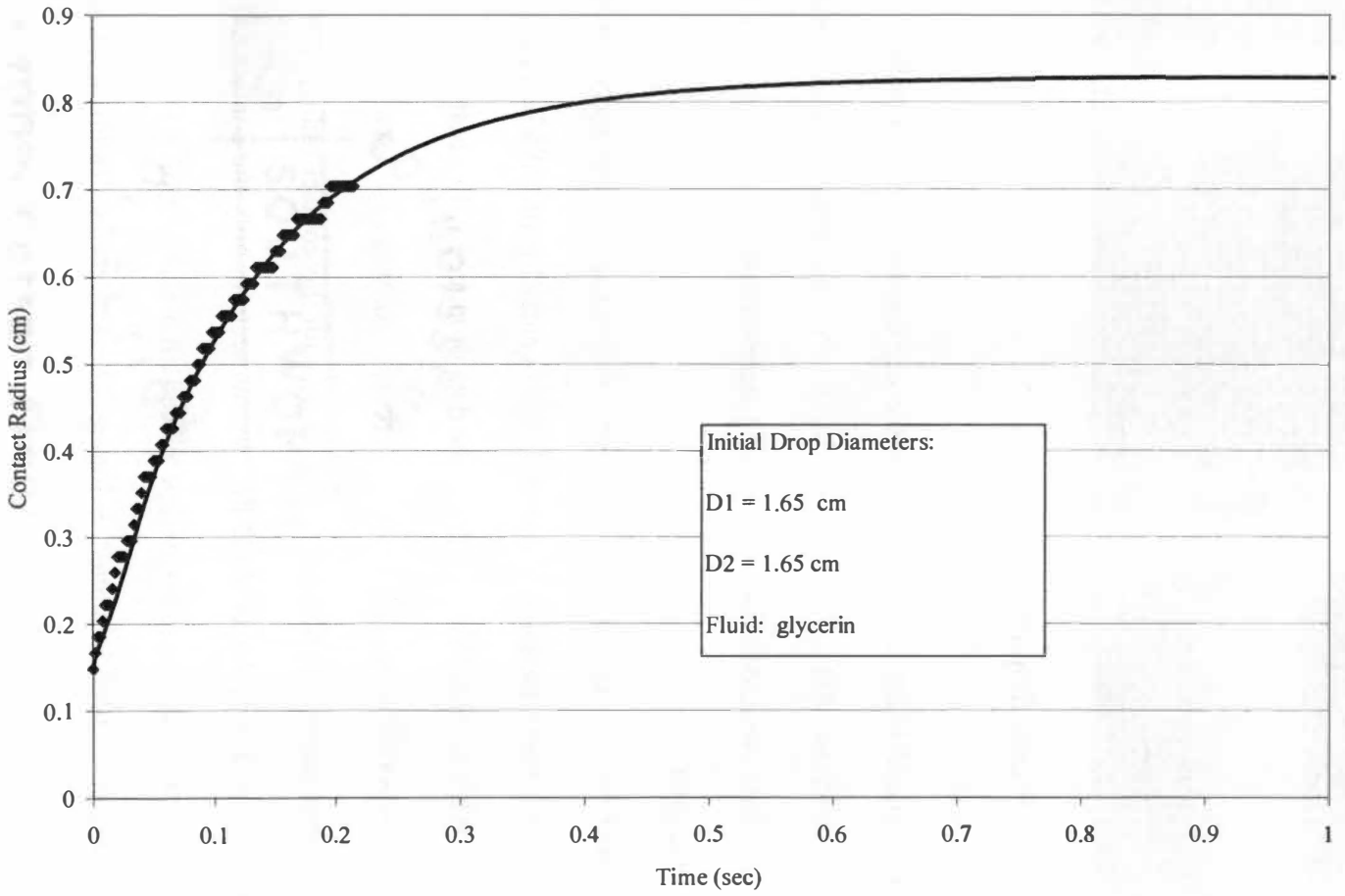


Figure 20. Determining Time Scale by Matching Curves of the Growth of the Contact Radius of Two Initially Equal Droplets of Glycerin as the Droplets Merge with Sintering Computer Model for Cylinders with Radius Ratio of 1 to 1.

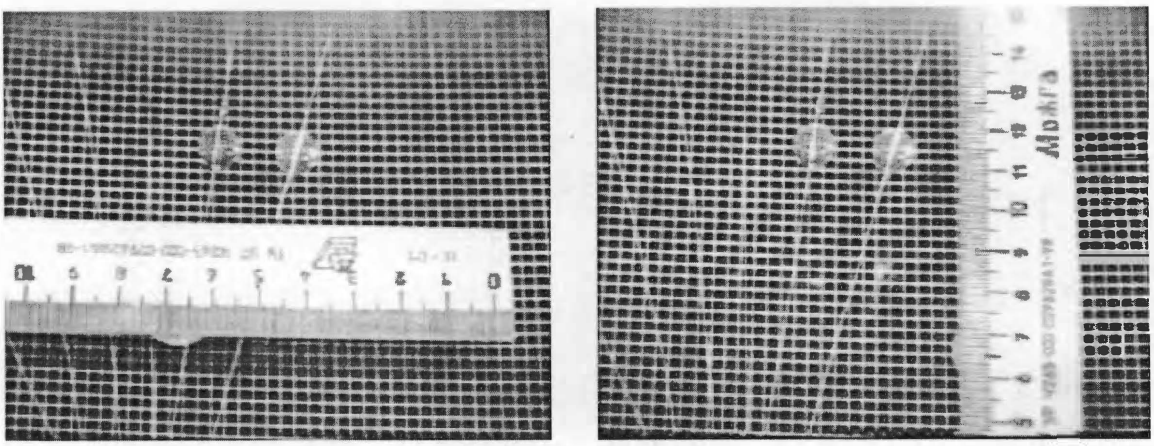


Figure 21. Calibration Photos from ISS Experiment.

of pixels was taken and divided by 1cm to give the calibration 23.5 pixels/cm. An average was needed because there was a slight distortion of the image due to camera angle. The average was centered around the area where coalescence occurred in the image to improve accuracy.

Experimental time was calculated in the same manner as before, with a frame speed of 30 frames per second, meaning that each frame occurred $1/30^{th}$ of a second after the previous frame. With the time and lengths of the data produced with Spotlight™, the raw data for the ISS experiment was plotted with Excel®. As was discussed earlier the data from unequal sized drops was plotted in two ways, with the contact radius, such as we did for equal drops, and with the axial widths. In this section, only the contact radius plots will be used; the axial width graphs will be placed after this section. The data for the contact radius change in time is plotted in Figure 22. The contact radius evolution data is limited, however, due to the increasing difficulty in determining exactly the value of the contact radius after the boundary of the merging drops loses a distinct dip.

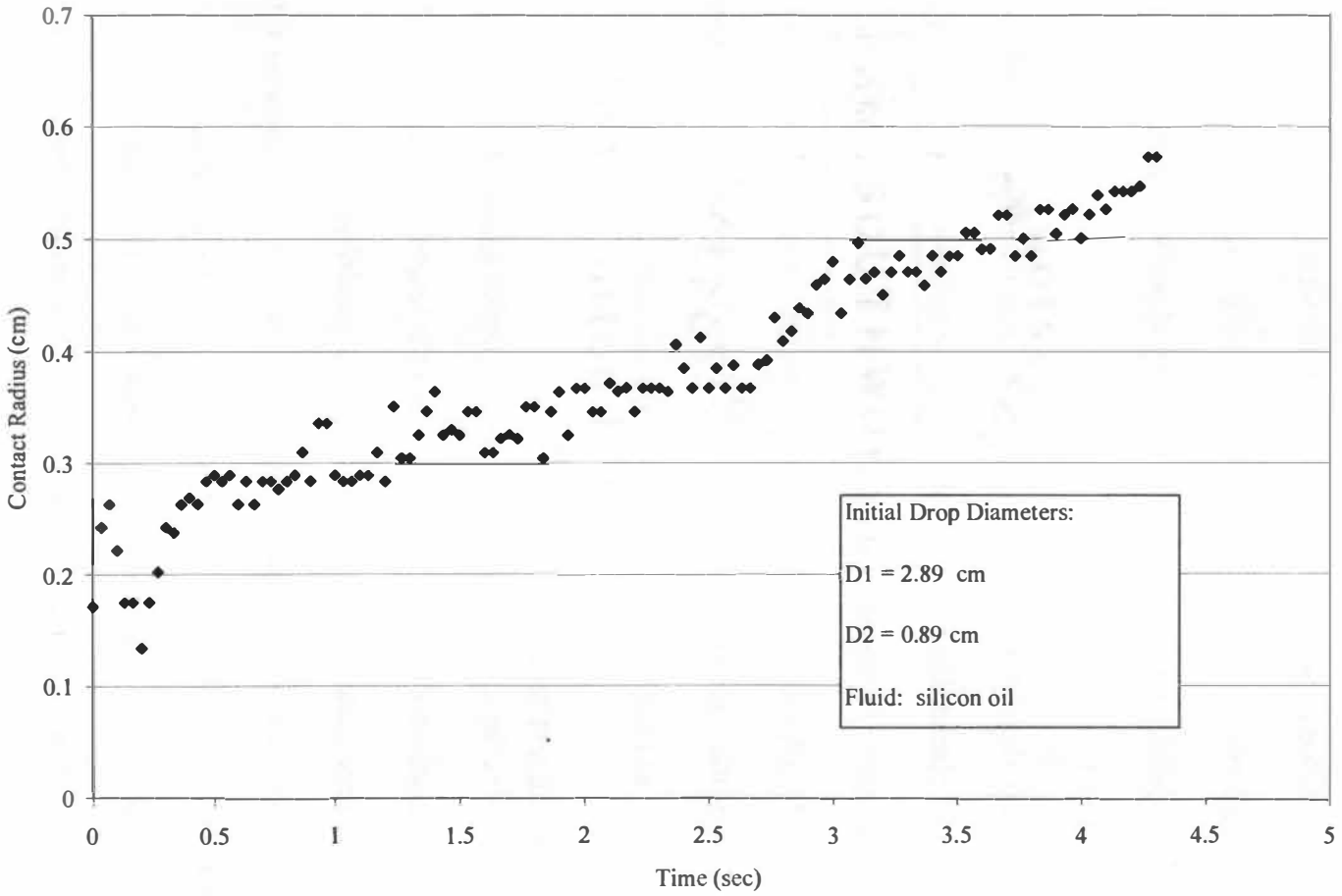


Figure 22. Experimental Contact Radius Raw Data from ISS Experiment for the Merging of Two Unequal Diameter Drops of Silicon Oil.

MODEL CURVE

A major difference between this experiment and the KC-135 experiment was the ratio of the drop diameters that were merged. For the ISS experiment drops of two different sizes were coalesced. Spotlight™ was used here as well to measure the size of the drops before coalescence started. We set the large drop's radius to 1 l^* and the smaller drop is simply the size ratio that we obtain from Spotlight™. The ratio found for the sequence was 0.31 to 1.

We again placed this ratio into our Initial Value program, obtained the initial geometry from that and placed this geometry into the single symmetry sintering program and ran model. The graph of the model contact radius versus time is plotted in Figure 23. The non-dimensional length again is converted by finding the physical length scale by measuring the radius of the large circle, giving a value of l_s=1.425 cm. From the known length scale we can proceed to find the time scale and the viscosity value.

VISCOSITY MEASURED

The raw data curve for the ISS contact radius was plotted against the model curve in Figure 24. As discussed above we have already found the length scale and the surface tension is known; the time scale is the only unknown in determining the viscosity. The time scale was varied in Excel® until the two curves matched up. The value of t_s that produced the best fit was 7.9 seconds, which when placed into our equation gives a viscosity of 119 dyne·s/cm. Two other time scales are shown on Figure 24, ts = 5 and ts =2 with respective viscosities of 75 and 30 dyne·s/cm. The nominal viscosity of this silicon oil is 125 dyne·s/cm.

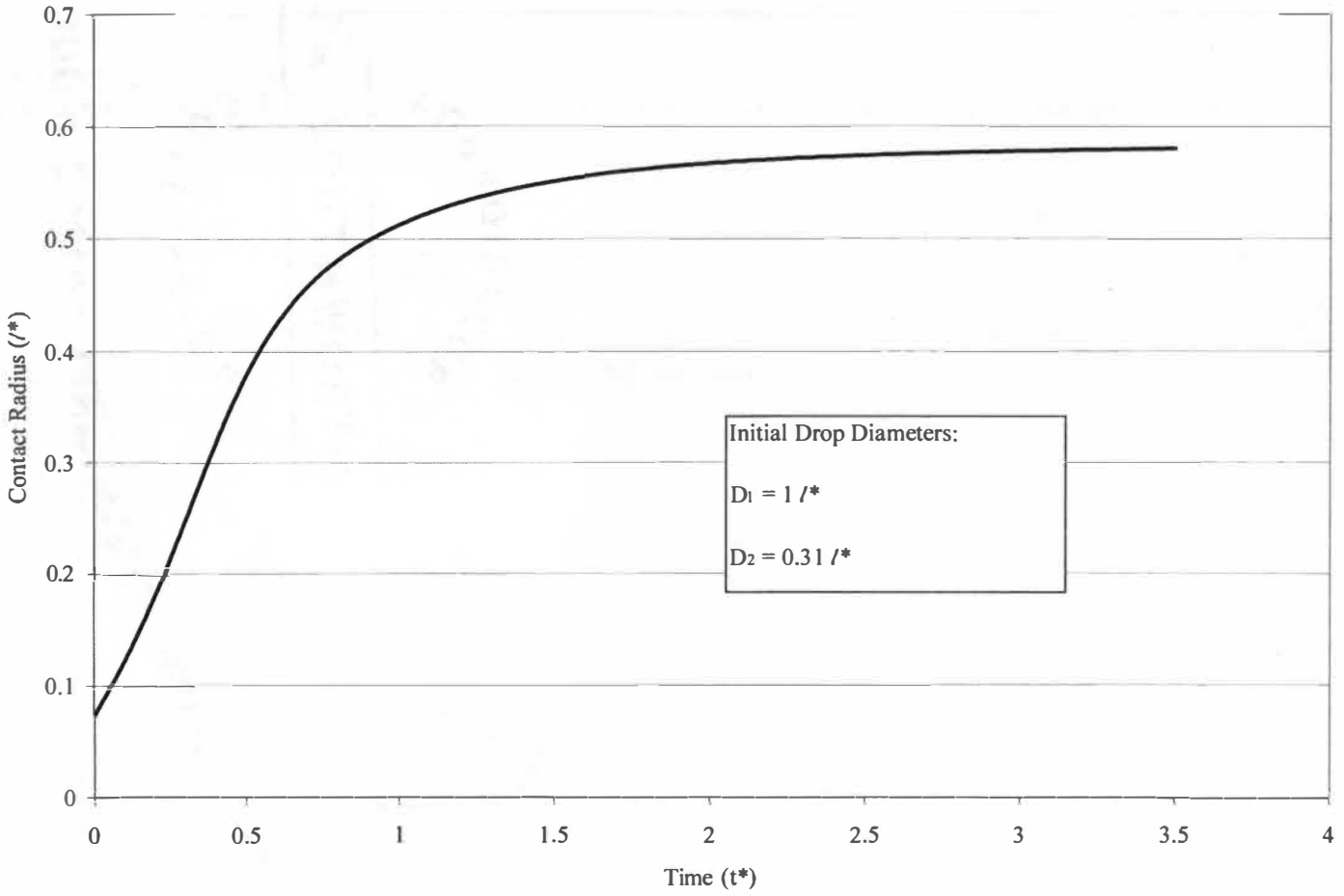


Figure 23. Model Contact Radius Variation for Initial Droplet Diameter Ratio of 0.31 to 1.

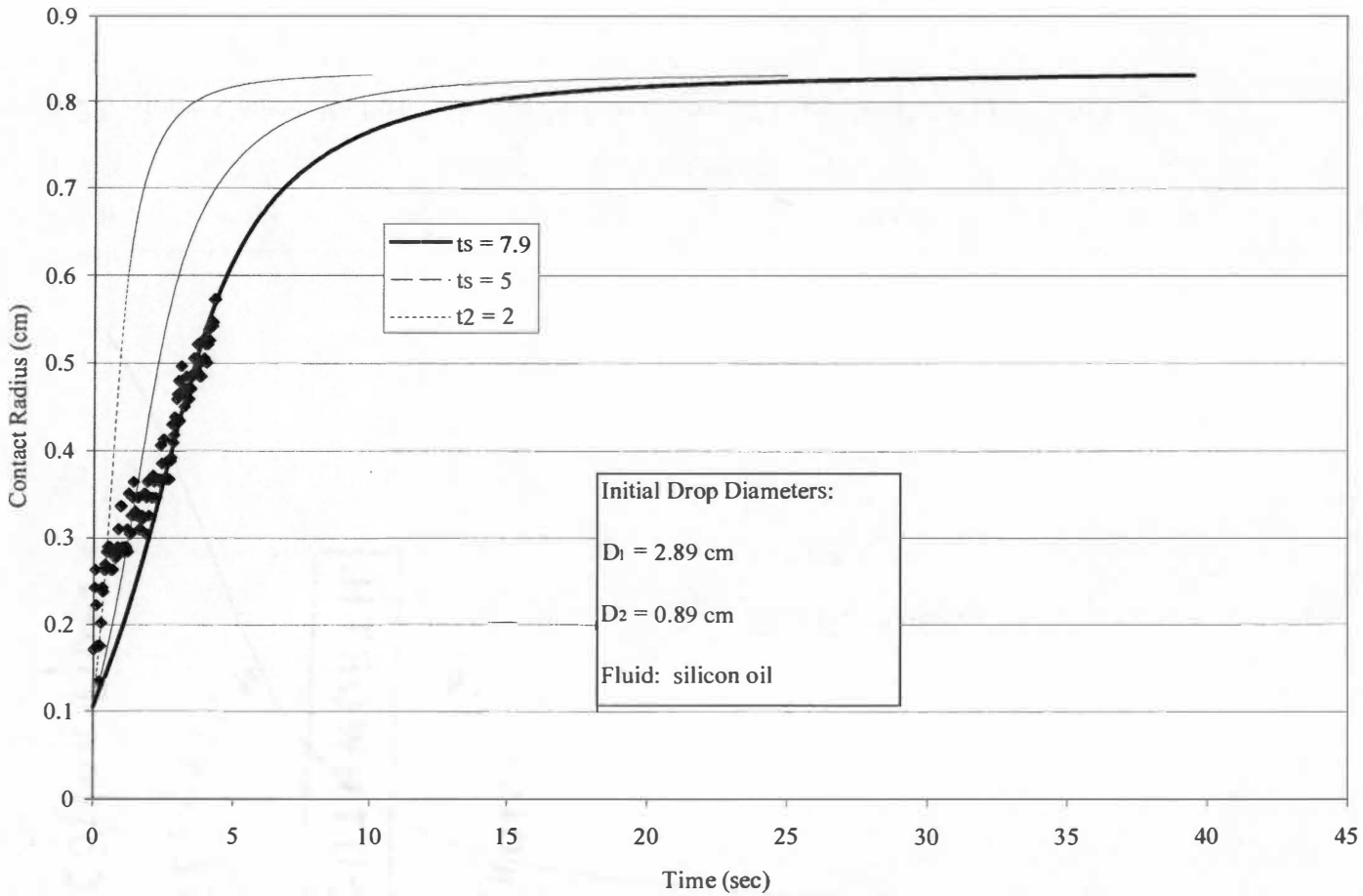


Figure 24. Comparison of Multiple Time Scales for the Growth of Contact Radius with the Experimental Merger of Two Drops of Unequal Diameter.

AXIAL WIDTH

The data presented for the axial width was deduced from the same ISS-produced video as the contact radius. The difference, however, is that the data points were taken from the outside edges of the merging drops system, instead of the contact radius. This means that the same calibration of 23.5 pixels/cm and 1 frame / 30 frame per second can be used to present the data in engineering units. The axial width raw data is presented in Figure 25 below.

One main feature that stands out when looking at the data is a hump at the beginning of the merging. This hump, expanded in Figure 26, represents a slight repulsion of the two drops before coalescence takes place, although we are not yet certain what causes this phenomena. This was seen in the computer model, but dismissed as errors in initial values until it was seen in the actual experiment.

Another important feature in the plot is an interval where the data is not smooth. This is attributed to the string being tugged on slightly during the experiment. This temporarily interrupted the coalescence process and will need to be taken into consideration when curve matching is performed.

The computer model that was used to give the contact radius progression from the previous section also provided the time-variation of the axial width. This curve is shown in Figure 27 with general scaling to provide accurate units. To match up the curves we can place in the same length scale from the previous, 1.425cm. However, a different time scale is needed. Figure 28 shows a variety of time scale possibilities, t_s=2.7 matches the beginning of the curve the best. This is the part that was not distorted.

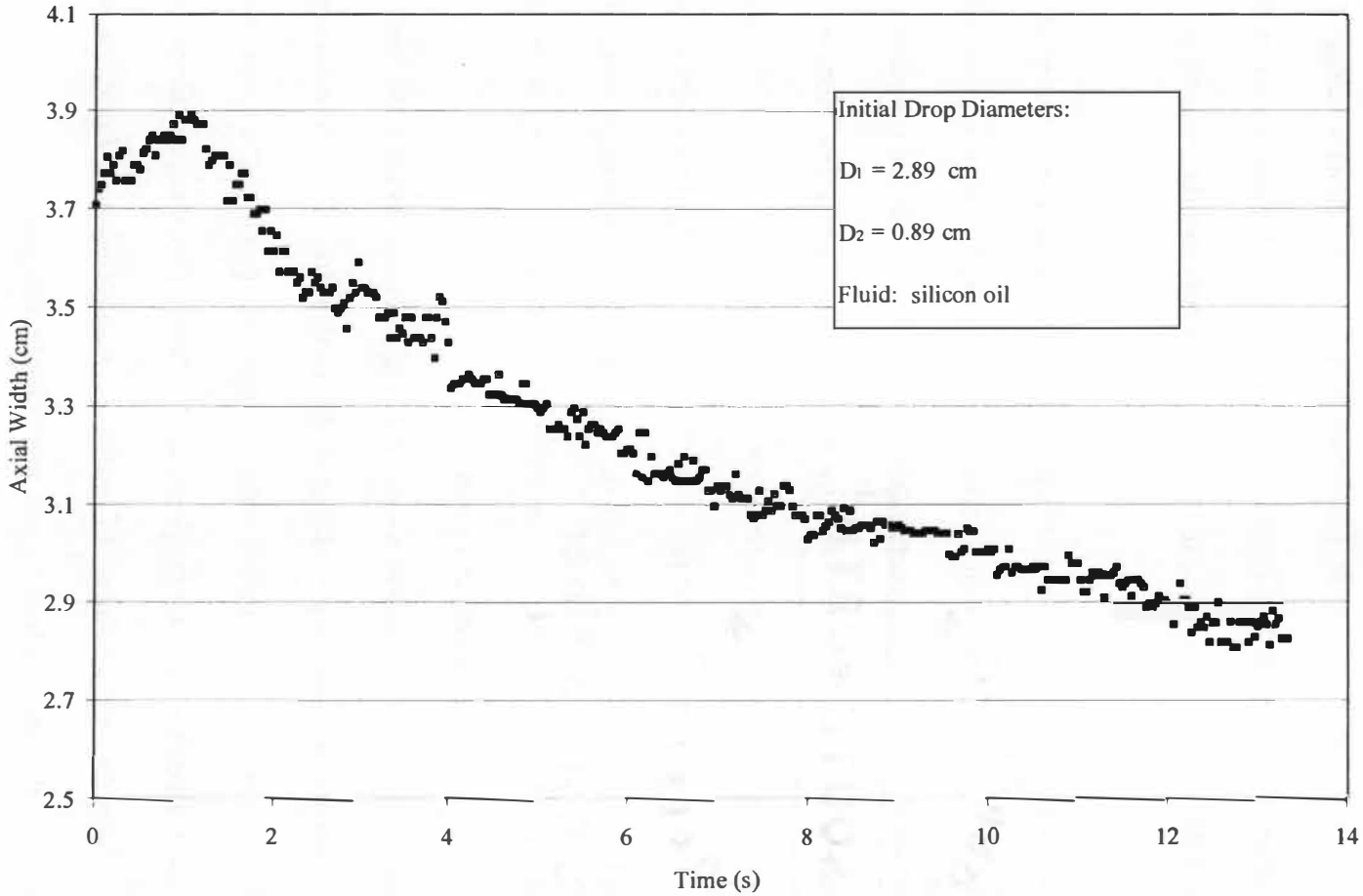


Figure 25. Experimental Data on the Axial Width of Merging Droplet Pairs During Coalescence.

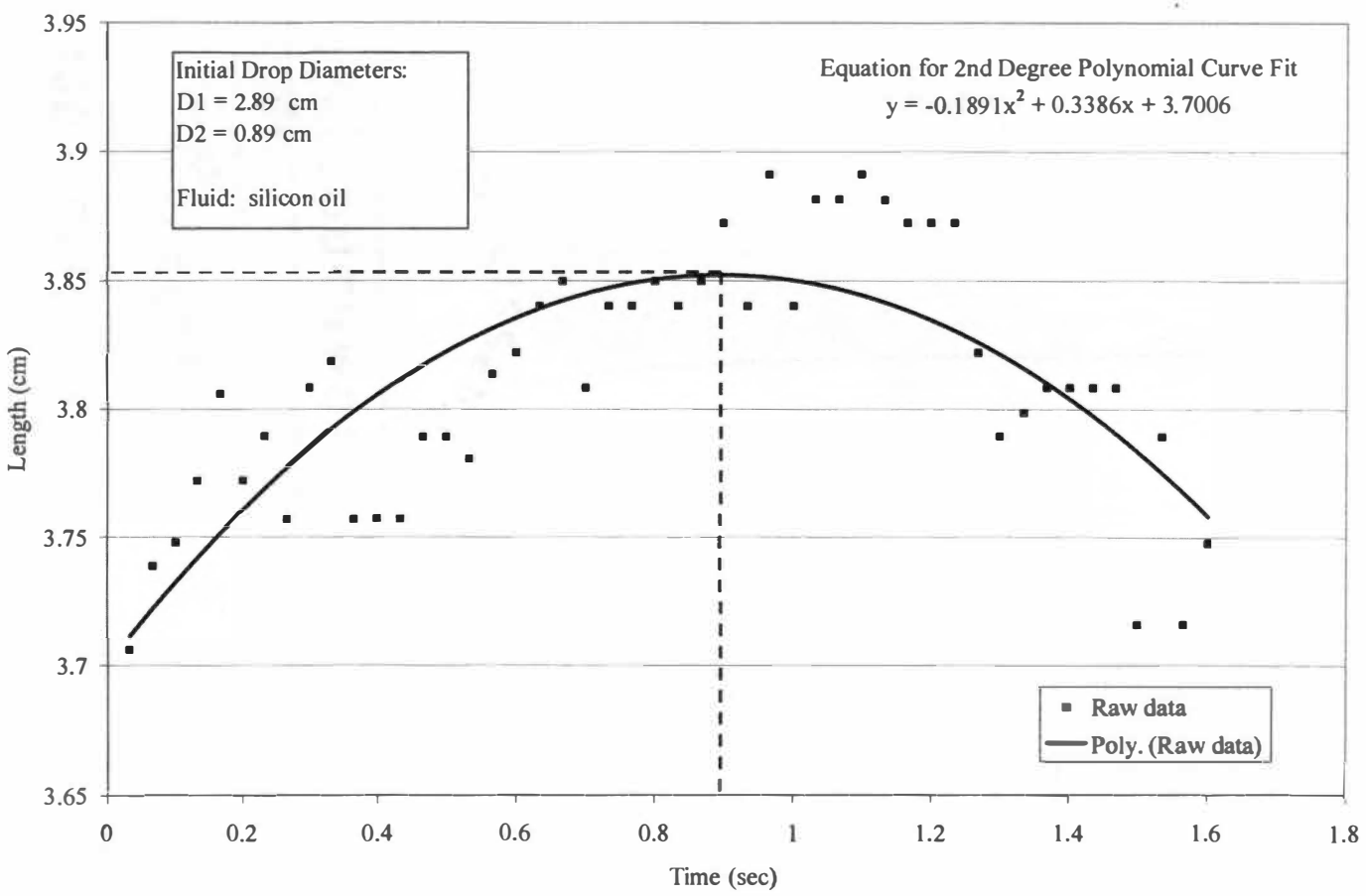


Figure 26. Experimental Data on the Axial Width of Merging Droplet Pairs During Coalescence: Concentrated Time Axis with Local 2nd Degree Polynomial Curve Fit of the Data.

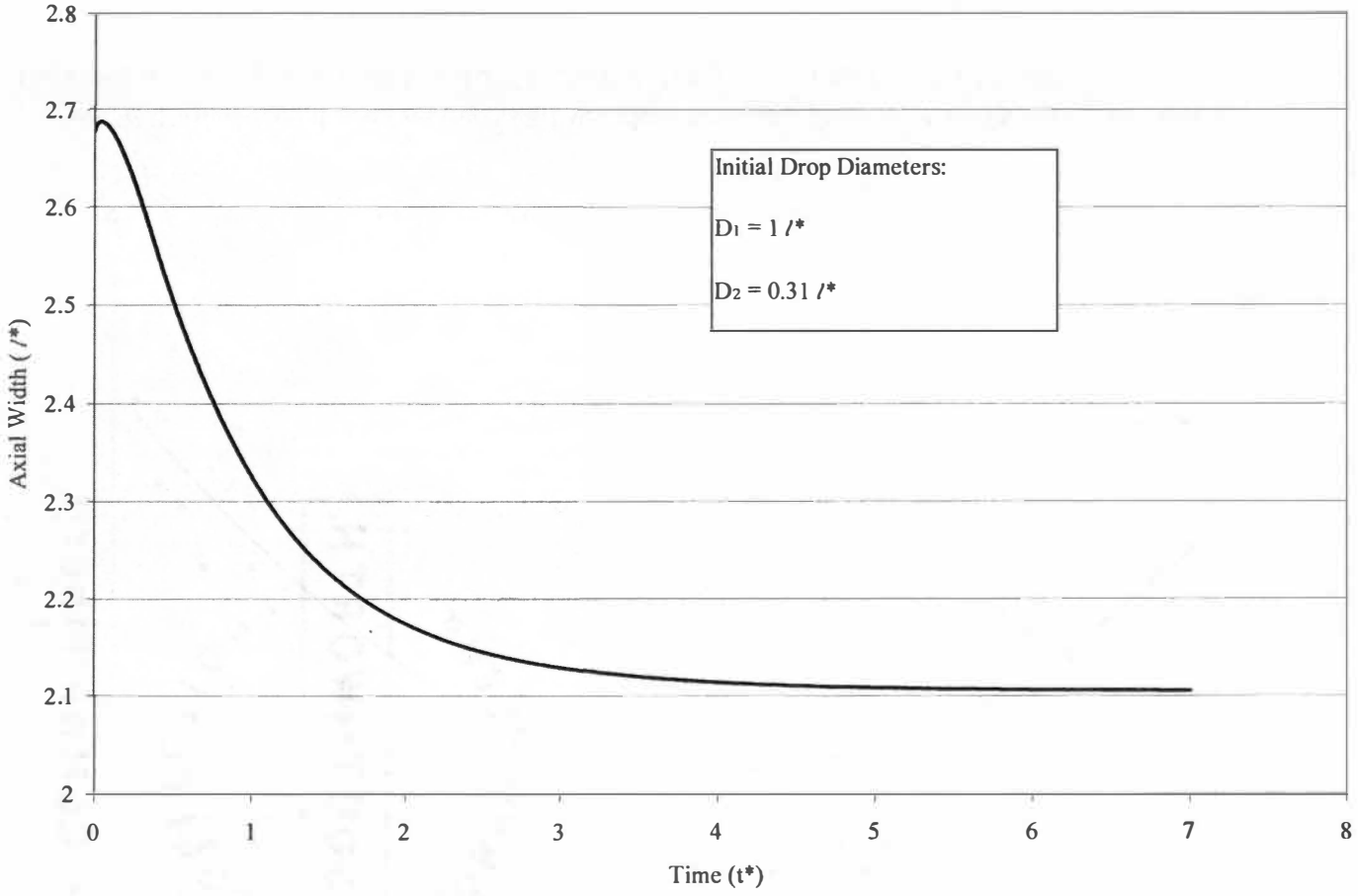


Figure 27. Model Axial Width of Merging Droplet Pairs During Coalescence.

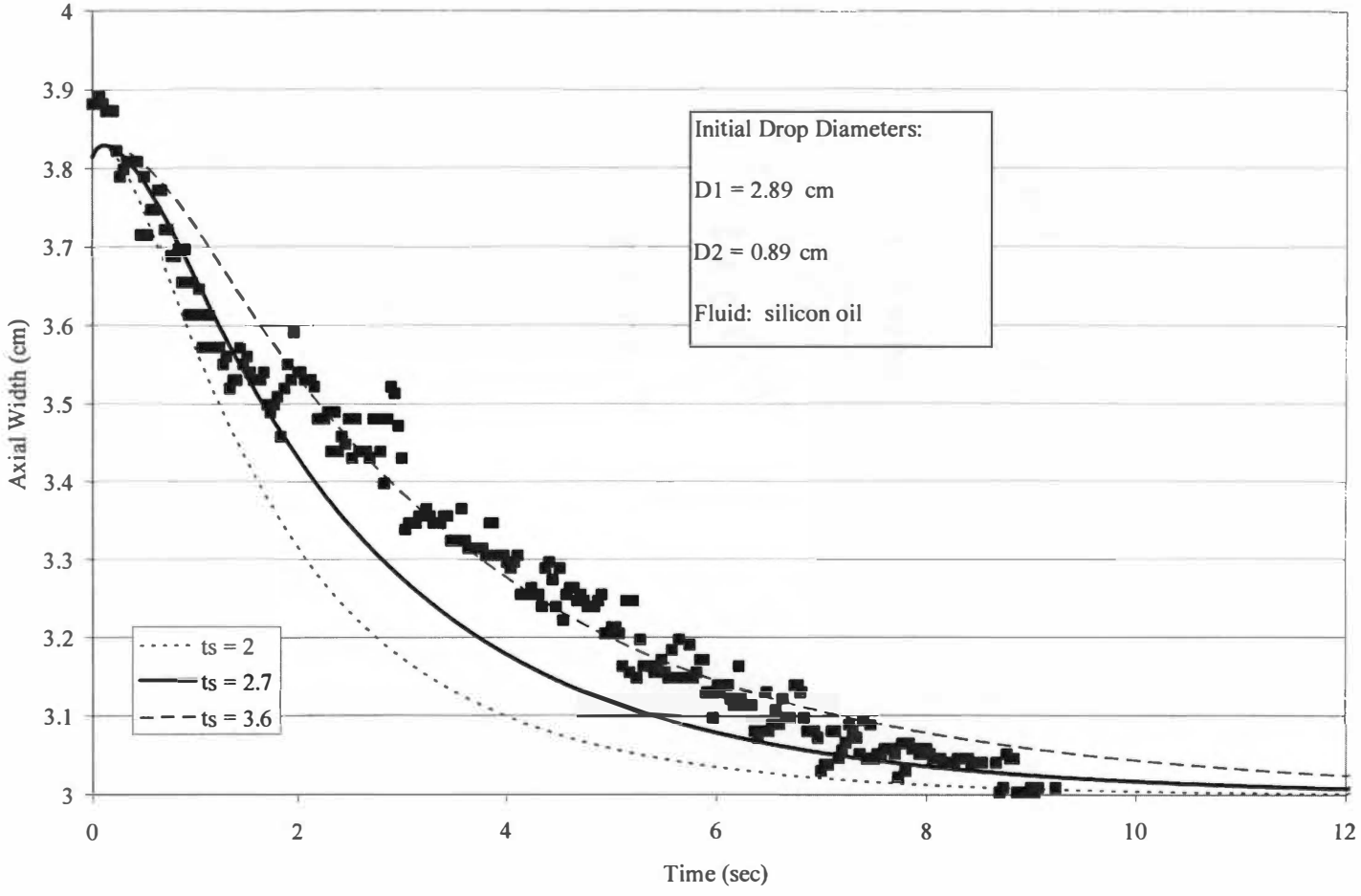


Figure 28. Comparison of Multiple Time Scales on the Change of Axial Width with the Experimental Merger of Two Drops of Unequal Initial Diameter.

CHAPTER 6: CONCLUSIONS AND RECOMMENDATIONS FOR FUTURE WORK

Two different liquids with different properties and different initial diameter ratios were experimentally tested by droplet merging experiments in two different microgravity environments. Both sets of experiments yielded fairly accurate estimates of viscosity for liquids of known viscosities. Measuring the contact radius progression with time has proven to be very useful for finding this value. This implies that if we could use this method with the liquids where we do not know the value of the viscosity that we would be able to estimate their viscosities to within 5% based on the results of these tests. Even an order of magnitude estimate would allow scientists to improve their mathematical models. Improvements in these estimates would be provided by using the sintering computer model with spherical drops in place of the cylindrical two-dimensional mdel.

The ultimate goal of this study is to develop a method to obtain values of viscosity for undercooled liquid glasses. To ensure that this method is suitable for this purpose, future tests should include testing materials of known viscosities in the range that we expect to find these glass transition materials, 10^1 to 10^6 Poise. Other tests should be performed on liquids at approximately the same temperature as those needed, above 850K. To do this a containerless positioning furnace would have to be used.

Points of interest that can be worked on in the future is determining why the axial width needs a different time scale for the same graphical information. Whether it is due to the fact that a two-dimensional computer model was used or due to the size difference of the two drops. To answer this question more tests based on drops of different ratios

will need to be performed, as well as performing the axial width calculation on drops of equal diameters. Testing different viscosities would also prove useful in determining this as a factor. Along with the time scale of the axial width, the repulsion that was seen is of interest. Further thought and research will go into this phenomenon.

REFERENCES

Antar, Basil N., Etheridge, Edwin C., and Maxwell, Daniel (1999). Utilization of Low Gravity Environment for Measuring the Viscosity of Highly Viscous Liquids. Advanced Space Research, 24 (10), 1289-1292.

Antar, Basil N., Etheridge, Edwin C., and Maxwell, Daniel (2003). Viscosity Measurement using Drop Coalescence in Microgravity. Microgravity Science and Technology, XIV/1, 9-19.

Becker, A. A. (1992). The Boundary Element Method in Engineering. McGraw-Hill

More Solutions to Sticky Problems. Brookfield Engineering. <http://www.brookfieldengineering.com/support/viscosity/index.cfm> (21 May 2005).

Callister, William D., Jr. (2000). Materials Science and Engineering (5th ed.). New York: John Wiley & Sons, Inc.

Etheridge, E., Antar, B., and Maxwell, D. (1999). Viscosity Measurement of Highly Viscous Liquids Using Drop Coalescence in Low Gravity. 37th AIAA Aerospace Sciences Meeting and Exhibit January 11-14, 1999 / Reno, NV

Frenkel, J. (1945). Viscous Flow of Crystalline Bodies under the Action of Surface Tension. Journal of Physics, 9. 385

Happel, J., Brenner, H. (1965). Low Reynolds Number Hydrodynamics. Englewood Cliffs, NJ: Prentice Hall.

Hopper, R. W. (1984). Coalescence of Two Equal Cylinders: Exact Results for Creeping Viscous Plane Flow Driven by Capillarity. Community of American Ceramic Society. C-263

Hopper, R. W. (1990). Plane Stokes Flow Driven by Capillarity on a Free Surface. Journal of Fluid Mechanics, 213. 349

Hopper, R. W. (1991). Plane Stokes Flow Driven by Capillarity on a Free Surface: 2. Further Developments. Journal of Fluid Mechanics, 230. 335

Klimek, Robert (2004, May). Software for Analyzing Sequences of Flow-Related Images NASA Tech Brief. < http://www.nasatech.com/Briefs/cs.html> (5 Aug 2004).

Naka, M., Nishi, Y., and Masumoto, T. (1978). Proceedings of the Third International Conference on Rapidly Quenched Metals (Vol. I). London: Metals Society.

Panton, Ronald L. (1996). Incompressible Flow (2nd ed.). New York: Wiley.

Pnueli, David and Gutfinger, Chaim (1992). Fluid Mechanics. Cambridge: Cambridge University Press.

Pokluda, Ondrej, Bellehumeur, Celine T., and Vlachopoulos, John (1997, December). Modification of Frenkel's Model for Sintering. AIChE Journal, 43 12, 3253-32569.

Schlichting, Herman and Truckenbrodt, Erich (2001). Aerodynamik des Flugzeuges. Heidelberg: Springer.

Vorst van de, G. A. L., Mattheij, R. M. M., and Kuiken, H. K. (1992). A Boundary Element for Two-Dimensional Viscous Sintering. Journal of Computational Physical 100, 50-63

Vorst van de, G. A. L., Mattheij. R. M. M. (1995). Simulations of Viscous Sintering in Boundary Element Applications in Fluid Mechanics. South Hampton and Boston: Computational Mechanics Publications.

Walls, Bryan, A Selected Glossary of Science Terms, NASA Marshall Space Flight Center. < http://science.nasa.gov/newhome/help/glossary.htm> (21 July 2005).

Young, Donald F., Munson, Bruce R., and Okiishi, Theodore H. (2001). A Brief Introduction to Fluid Mechanics. (2nd ed.). New York: Wiley

APPENDIX

APPENDIX A

NON-DIMENSIONAL ANALYSIS

Parameters Involved in dimensions of Force (F), Length (L), and Time (T).

	V	μ	σ	P	L	T
F	0	1	1	1	0	0
L	1	-2	-1	-2	1	0
T	-1	1	0	0	0	1

Want V, P, and T as f(μ, σ, and L).

Π_1 V μ σ L

$(LT^{-1})(FL^{-2}T)^a(FL\text{-}1)^b(L)^c \doteq F^0L^0T^0$

F: $0 + a + b = 0 \rightarrow a = -b \rightarrow \underline{b = -1}$

L: $1 - 2a - b + c = 0 \rightarrow c = 2a + b - 1 = 2 - 1 - 1 \rightarrow \underline{c = 0}$

T: $-1 + a = 0 \rightarrow \underline{a = 1}$

$$\Pi_1 = \frac{V\mu}{\sigma} \rightarrow \boxed{V = \frac{\sigma}{\mu}}$$

Π_2 P μ σ L

$(FL^{-2})(FL^{-2}T)^a(FL\text{-}1)^b(L)^c \doteq F^0L^0T^0$

F: $1 + a + b = 0 \rightarrow b = -1 - a \rightarrow \underline{b = -1}$

L: $-2 - 2a - b + c = 0 \rightarrow c = 2 + b = 2 - 1 \rightarrow \underline{c = 1}$

T: $\underline{a = 0}$

$$\Pi_2 = \frac{PL}{\sigma} \rightarrow \boxed{P = \frac{\sigma}{L}}$$

Π_3 T μ σ L

$(T)(FL^{-2}T)^a(FL\text{-}1)^b(L)^c \doteq F^0L^0T^0$

F: $0 + a + b = 0 \rightarrow b = -a \rightarrow \underline{b = 1}$

L: $0 - 2a - b + c = 0 \rightarrow c = 2a + b = 2a - a = a \rightarrow \underline{c = -1}$

T: $1 + a = 0 \rightarrow \underline{a = -1}$

$$\Pi_3 = \frac{T\sigma}{\mu L} \rightarrow \boxed{T = \frac{\mu L}{\sigma}}$$

APPENDIX B

INITIAL VALUE GENERATOR

```
/***************************************************************************
                          initval.cpp  -  description
                             -------------------
    begin                : Wed Jan 14 13:16:48 CST 2004
    copyright            : (C) |2004| by Daniel Lehman
***************************************************************************/

/***************************************************************************
 *   This is an initial value generator for the sintering programs         *
 *   Changes can be made to the radius, gap size, and number               *
 *    of initial values.                                                   *
 ***************************************************************************/

#ifdef HAVE_CONFIG_H
#include <config.h>
#endif

#include <iostream>
#include <cmath>
using namespace std;
#include <fstream>

ofstream out_file;

int main()
{
  const double alpha = M_PI/16.0;   //Sets the Contact Radius size
  const double rad1 = 0.5;          //Size of the right (+x) circle
  const double rad2 = 1.0;          //Size of the left (-x) circle
  const double start1 = 3.0*M_PI/2.0 - alpha;
  const double end1 = -M_PI/2.0 + alpha;
  const double beta = asin(sin(alpha)*rad1/rad2);
  const double start2 = M_PI/2.0 - beta;
  const double end2 = -3.0*M_PI/2.0 + beta;
  const double delta1 = (end1 - start1)/34.0;    // Discretization
  const double delta2 = (end2 - start2)/68.0;    // Number of Nodes
  const double ytop = rad1*cos(alpha);
  const double ybot = -rad2*cos(beta);

  int i;
  double x[102], y[102];      //Number of Nodes in Full Circle
  for(i=1; i <= 35; i++)      //Output of (+x) cirlce
  {
    x[i] = cos(start1 + (i-1)*delta1)*rad1;
    y[i] = ytop + sin(start1 + (i-1)*delta1)*rad1;
  }
  for(i=36;i<=102;i++)        //Output of (-x) circle
  {
    x[i] = cos(start2 + (i-35)*delta2)*rad2;
    y[i] = ybot + sin(start2 + (i-35)*delta2)*rad2;
  }

  out_file.open("start.dat",ios::app);          //File for output
  for(i=1;i<=102;i++)
  {
```

```
    out_file << x[i] << endl;
  }
  out_file << endl;
  for(i=1;i<=102;i++)
  {
    out_file << y[i] << endl;
  }

  out_file.close();
  return 0;
}
```

VITA

Daniel Lehman was born in a small town in South Dakota to Floyd and Sylvia Lehman. He was the youngest of three boys. Raised on a farm until the age of 3, he then moved to the sprawling urban area of Watertown, SD, with a population 20,000. Through his education Daniel was privileged to experience many unique opportunities such as traveling to several foreign countries while playing in a traveling symphony. At the age of 18, Daniel moved to Minneapolis Minnesota to pursue a bachelor's degree at the University of Minnesota. In 2003, he received that Bachelor's Degree in Aerospace Engineering with a minor in Astrophysics.

His love of space and lack of money brought him to graduate school at the University of Tennessee Space Institute. At UTSI Daniel received many more wondrous opportunities, including receiving his private pilot's license. With his professor Dr. Antar, Daniel has had the chance to fly multiple experiments aboard an aircraft that simulates zero gravity. He has also been a part of an experiment that was performed aboard the International Space Station and was privileged to watch it live as it happened. Where life will take Daniel next is uncertain, but the journey is always the most exciting part of any trip.

7695 2036 10
03/08/06 MAR